Inorganic Chemistry

Article

pubs.acs.org/IC

Synthesis, Characterization, and Photophysical Properties of Heteroleptic Copper(I) Complexes with Functionalized 3-(2′-Pyridyl)-1,2,4-triazole Chelating Ligands

Jing-Lin Chen,*[,†,‡] Xing-Fu Cao,[†] Jin-Yun Wang,*[,‡] Li-Hua He,[†] Zong-Yong Liu,[†] He-Rui Wen,[†] and Zhong-Ning Chen[‡]

[†]School of Metallurgy and Chemical Engineering, Jiangxi University of Science and Technology, Ganzhou 341000, People's Republic of China

[‡]State Key Laboratory of Structural Chemistry, Fujian Institute of Research on the Structure of Matter, Chinese Academy of Sciences, Fuzhou 350002, People's Republic of China

Supporting Information

ABSTRACT: A new series of mononuclear copper(I) complexes (**1**–**9**) with functionalized 3-(2′-pyridyl)-1,2,4-triazole chelating ligands, as well as the halide and/or phosphine ancillary ligands, have been synthesized. Complexes **1**–**9** were fully characterized by elemental analysis, NMR spectroscopy, mass spectroscopy, electronic absorption spectroscopy, fluorescence spectroscopy, cyclic voltammetry, and X-ray crystallography (**1**–**8**). They adopt a distorted tetrahedral configuration, and are considerably air-stable in solid state and in solution. All these Cu(I) complexes display a comparatively weak low-energy absorption in CH_2Cl_2 solution, assigned to charge-transfer transitions with appreciable MLCT character, as supported by TD-DFT studies. Cu(I) halide complexes **1**–**4** each shows bright solid-state emission at room temperature, although they are nonemissive in fluid solutions, in which the emission markedly depends on the halide and the substituent on the 2-pyridyl ring. Complexes **5**–**9** bearing 2-pyridyl functionalized 1,2,4-triazole and phosphine exhibit good photoluminescence properties in solution and solid states at ambient temperature, which are well-modulated via the alteration of the auxiliary phosphine ligand and the structural modification of 3-(2′-pyridyl)-1,2,4-triazole. Interestingly, cationic complex **6** and neutral derivative **7** can readily be interconverted through the ring inversion of the 1,2,4-triazolyl regulated by the NH ↔ N^- transformation.

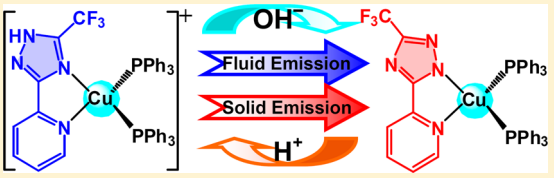

INTRODUCTION

There has been a rapidly growing interest in emissive transition-metal complexes, because of their potential applications in organic light-emitting devices (OLEDs), light-emitting electrochemical cells (LECs), chemical sensors/probes, and biological labeling.[1] With a focus on developing various luminous devices, great efforts have been devoted to the design and synthesis of transition metal-based phosphors with emission wavelengths in the entire visible spectral region,[2] especially the luminophores based on late transition-metal complexes. The most recognizable paradigms involve d^6 and d^8 complexes of the third-row transition series such as Os(II), Ir(III), and Pt(II).[3] However, because of the high cost and limited availability of these noble metals, more and more attention has been paid to the exploitation of inexpensive alternatives over the past two decades.[4] Copper(I) systems currently have become an important class of luminescent metal complexes, based on their relative abundance, low cost, and ability to display the promising application perspectives in optoelectronics.[5] In this field, the phosphine-containing copper(I) complexes are probably most widely studied,[6] among which heteroleptic Cu(I) complexes with the bidentate ligands (diimine and/or diphosphine) have attracted recent interest,[7] and a limited number of OLEDs doped with such emitters have been investigated.[8] In 2005, Harkins and Peters reported a dicopper(I) complex supported by a rigid, bulky PNP ligand (PNP = bis(2-diisobutylphosphinophenyl)amide), which exhibited an unusually high quantum yield and long-lived excited state.[9] Recently, the OLED fabricated with the above optimized analogue $\{(PNP\text{-}^tBu)Cu^I\}_2$ (PNP-^{t}Bu$^-$ = bis(2-diisobutylphosphino-4-*tert*-butylphenyl)amido) showed a 16% external quantum efficiency.[10] In 2011, Hashimoto and co-workers reported a series of highly emissive three-coordinate copper(I) complexes Cu(dtpb)X (dtpb = 1,2-bis(*o*-ditolylphosphino)benzene; X = I, Br, Cl), in which a vapor-deposited OLED doped with Cu(dtpb)Br exhibited a maximum external quantum efficiency of 21.3%.[11]

With respect to $[Cu(N\text{^}N)(P_2)]^{+/0}$ system (N^N = diimine, P_2 = diphosphine or two monophosphine),[12] the highest occupied molecular orbital (HOMO) has a dominant metal d(Cu) character, probably mixed with some contribution of the phosphine ligand, while the lowest unoccupied molecular orbital (LUMO) is basically resident on the diimine ligand. Thus, the emission corresponding to the lowest triplet excited state is essentially ascribed to the metal-to-ligand charge

Received: February 3, 2013

   dx.doi.org/10.1021/ic4002829 | *Inorg. Chem.* XXXX, XXX, XXX–XXX

transfer (^{3}MLCT) transition, which is normally sensitive to coordination environment and peripheral ligand. It is shown that the use of sterically congested ligands forms a rigid environment around the Cu(I) center, and hence effectively suppresses the nonradiative processes caused by Jahn−Teller distortion and ligand dissociation of emissive states as well as solvent-induced exciplex formation.[13] Furthermore, because of the low oxidation potential of the Cu(I) core and the absence of a higher-lying metal centered d−d state induced emission quenching, Cu(I) complexes are thus able to yield efficient emission and are highly desirable for the fabrication of both OLEDs[14] and LECs[15] with relatively low cost, compared to Ru(II), Os(II), Ir(III), and Pt(II) metal complexes. Another important advantage of Cu(I) complexes, in comparison to the late transition-metal complexes, is more environmentally benign. It is worthy of note that ionic emissive species can be utilized as the electronically active component of the electroluminescent layers of LECs to generate efficient light output.

In sharp contrast to the $[Cu(N^N)(P_2)]^{+/0}$ species, neutral heteroleptic complexes Cu(N^N)(P)X (N^N = diimine, P = monophosphine, X = halogen or pseudo-halogen) have been much less investigated,[16] despite the fact that they should more easily undergo the vacuum deposition process in the fabrication of electroluminescence devices. In fact, only a limited number of reports involving emissive properties of Cu(dipyrido[3,2,-a:2′,3′-c]phenazine)(PPh_3)I, Cu(N,N)(PR_3)(NCS) (N,N = phen, 2,2′-bpy, two py), Cu(6-cyano-2,2′-bipyridine)(PPh_3)X (X = I, Br), and Cu(2-{2-benzimidazoly}-6-methylpyridine)-(PPh_3)X (X = I, Br, Cl) complexes have been described.[17]

In pursuit of novel emissive Cu(I) complexes, structural modification of commonly used ligands such as 2,2′-bipyridine or phenanthroline is an effective approach, while another alternative route involves the utilization of previously unemployed ligands. Several studies on the coordination chemistry of triazoles and their chelating derivatives have been reported recently.[18] The 1,2,3-triazole-based chelating ligands have been employed most recently for the construction of emissive Cu(I) complexes.[19] Of 3,5-disubstituted-1,2,4-triazole, 3-(2′-pyridyl)-1,2,4-triazoles have been used to synthesize photoactive Ru(II), Os(II), Ir(III), and Pt(II) metal complexes.[20] However, to the best of our knowledge, luminescent Cu(I) complexes bearing functionalized 3-(2′-pyridyl)-1,2,4-triazole and phosphine ligands have not been reported hitherto. Herein, we describe the synthesis, characterization, and photophysical properties of a novel class of emissive heteroleptic copper(I) complexes with tailorable 3-(2′-pyridyl)-1,2,4-triazole ligand (see Chart 1 and Scheme 1). It is

Chart 1

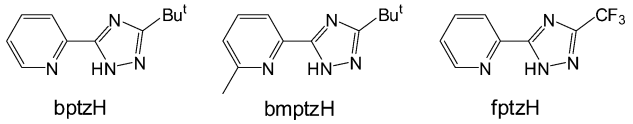

demonstrated that all these Cu(I) complexes with functionalized 3-(2′-pyridyl)-1,2,4-triazole are considerably air-stable in both solution and solid states, and they exhibit tunable emission properties that are markedly influenced by the variation of the ancillary ligand such as halide and phosphine as well as the structural modification of 3-(2′-pyridyl)-1,2,4-triazole. Interestingly, it is notable that the interconversion between cationic

Scheme 1. Structures of Mononuclear Cu(I) Complexes 1−9

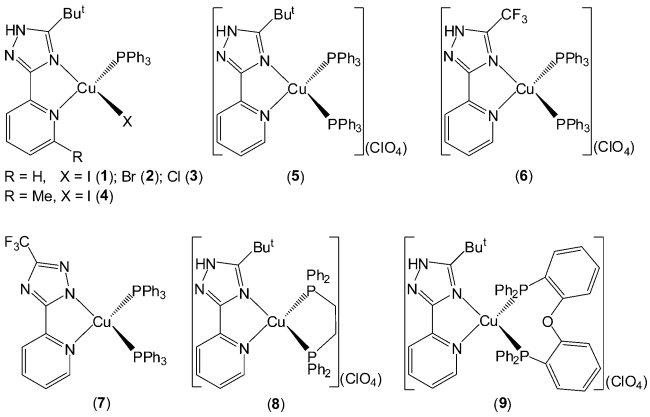

complex **6** and neutral derivative **7** can be successfully achieved via the ring inversion isomerism of the coordinated 1,2,4-triazolyl modulated by the controllable NH ↔ N$^-$ transformation. Complexes **6** and **7** show distinct photoluminescence properties in solution and in the solid state, in which neutral derivative **7** displays a blue-shifted fluid emission and a red-shifted solid-state emission, relative to the parent species **6**.

RESULTS AND DISCUSSION

Syntheses and Characterizations. Mononuclear copper(I) halide complexes **1**−**4** were first prepared by treatment of cuprous halide with 2 equiv of PPh_3 in CH_2Cl_2 solution, followed by the addition of 1 equiv of 5-*tert*-butyl-3-(2-pyridyl)-1H-1,2,4-triazole (bptzH) or 5-*tert*-butyl-3-(6-methyl-2-pyridyl)-1H-1,2,4-triazole (bmptzH). Halide complexes **1**−**4** are soluble in dimethylformamide (DMF) and dimethylsulfoxide (DMSO), but only sparingly soluble in CH_2Cl_2, $CHCl_3$, and CH_2ClCH_2Cl. In the ^{1}H NMR spectra of **1**−**4** in DMSO-d_6, besides the aromatic proton signals (δ 8.4−7.3 ppm) and the C−H resonances from the *tert*-butyl at 1.3 ppm and the methyl at 2.3 ppm as two singlet peaks, the characteristic N−H proton of the 1,2,4-triazolyl occurs at ∼14.4 ppm as a broad singlet peak, implying that the bmptzH and bptzH ligands coordinate to the Cu(I) center as a neutral ligand without the cleavage of the N−H bond, as revealed by X-ray crystallography. The ^{31}P{^{1}H} NMR spectra exhibit a broad singlet peak at −6.05, −5.23, −4.69, and −7.91 ppm for **1**−**4**, respectively, somewhat varying with both the halide ligand and the substituent on the 2-pyridyl. For halide complexes **1**−**4**, an intensive molecular ionic peak fragment (m/z, 527 or 541, $[M-X]^+$) is observed in their ESI mass spectra.

Complexes **5** and **6** were prepared by reaction of $[Cu(PPh_3)_2(CH_3CN)_2](ClO_4)$ with an equivalent amount of ligand bptzH and 5-trifluoromethyl-3-(2-pyridyl)-1,2,4-triazole (fptzH), respectively. Complexes **8** and **9** were accessible via the reaction of $[Cu(CH_3CN)_4](ClO_4)$ with bptzH and diphosphine (1,2-bis(diphenylphosphino)ethane (dppe) or bis[2-(diphenylphosphino)phenyl]ether (DPEphos)) in a 1:1:1 molar ratio. Neutral complex **7** was accessed by reacting $[Cu(PPh_3)_2(CH_3CN)_2](ClO_4)$ with 1 equiv of fptzH in the presence of NaOH. Interestingly, complex **7** could be also obtained by laying H_2O over the acetone solution of **6** in several days, suggesting that H_2O perhaps promoted the N−H bond cleavage. In addition, neutral complex **7** readily converted back to cationic complex **6** upon the addition of slightly excess 40% $HClO_4$ solution. In the ^{1}H NMR spectra, the unique N−H

dx.doi.org/10.1021/ic4002829 | Inorg. Chem. XXXX, XXX, XXX−XXX

signals of the 1,2,4-triazole rings appear at 14.4−14.9 ppm as a broad singlet peak for **5**, **6**, **8**, and **9**, indicating that bptzH and fptzH are still a neutral chelate without the N−H bond cleavage, as revealed by X-ray crystallography. Strikingly different from the above-mentioned complexes, the characteristic N−H proton signal of **7** derived from fptzH is not observed in its ^{1}H NMR spectrum, as a result of NH deprotonation of the 1,2,4-triazolyl. In the ^{31}P NMR spectra, a broad singlet peak is observed at −0.19, −2.81, −1.11, −7.41, and −13.53 ppm for **5**−**9**, respectively, markedly depending on both the phosphine ancillary ligand and the modification of 3-(2′-pyridyl)-1,2,4-triazole. In the ^{19}F NMR spectra, complexes **6** and **7** exhibit a singlet peak at −64.25 and −63.29 ppm, respectively, which are attributable to a combination of the ring inversion and the NH ↔ N$^-$ conversion of the 1,2,4-triazolyl. Moreover, in the ESI mass spectra, all cationic complexes **5**, **6**, **8**, and **9** give an intensive molecular ionic peak fragment $[M-ClO_4]^+$, while neutral complex **7** displays a molecular ionic peak fragment $[M+1]^+$.

The structures of **1**−**8** were established by X-ray crystallography (see Figures 1−3, as well as Figures S1−S5 in

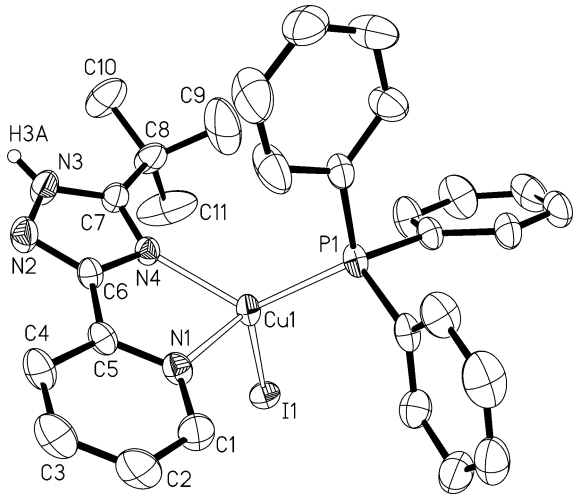

Figure 1. Perspective drawing of **1** showing 30% probability thermal ellipsoids and atom-labeling scheme. Hydrogen atoms except H3A are omitted for the sake of clarity.

the Supporting Information). The crystallographic data and structure refinement details of **1**−**4** and **5**−**8** are summarized in Tables 1 and 2, respectively. The selected bond lengths and angles are listed in Table 3 for **1**−**4** and Table 4 for **5**−**8**. Halide complexes **1**−**4** adopt an N_2PX distorted tetrahedral geometry around the Cu(I) center, in which bptzH or bmptzH displays a neutral chelating coordination mode. The Cu−$N_{pyridyl}$ lengths (2.1818(19), 2.189(3), and 2.195(4) Å for **1**, **2**, and **3**, respectively) are much longer than the Cu−$N_{triazolyl}$ lengths (2.0751(18), 2.082(3), and 2.087(4) Å for **1**, **2**, and **3**, respectively), showing a stronger bonding of the Cu(I) center to the N4 atom of the 1,2,4-triazolyl. Both Cu−$N_{pyridyl}$ and Cu−$N_{triazolyl}$ bonds of **1**−**3** are slightly elongated with the decrease of electron-donating ability of the halide (I^- > Br^- > Cl^-), implying that the halide possibly has some impact on the entire 3-(2′-pyridyl)-1,2,4-triazole ligand, and not simply on the pyridyl or 1,2,4-triazolyl fragment. Moreover, the Cu−P distances follow a ranking of **1** (2.2047(6) Å) > **2** (2.2022(11) Å) > **3** (2.1978(14) Å), suggesting that PPh_3 of

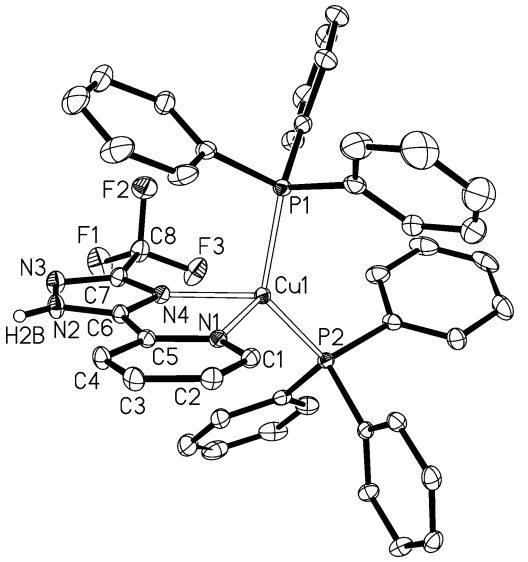

Figure 2. Perspective drawing of the cation of **6** showing 30% probability thermal ellipsoids and atom-labeling scheme. The ClO_4 anion and hydrogen atoms except H2B are omitted for the sake of clarity.

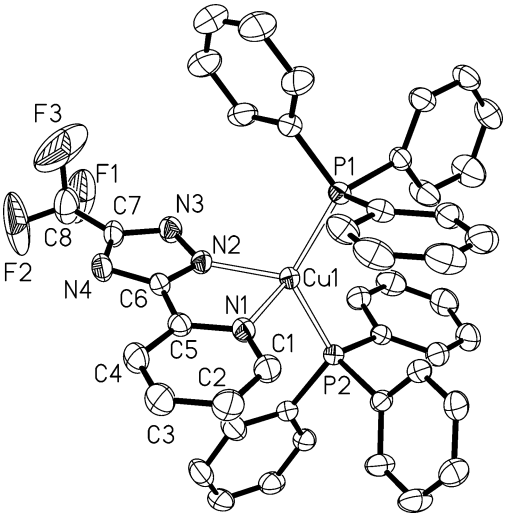

Figure 3. Perspective drawing of **7** showing 30% probability thermal ellipsoids and atom-labeling scheme. Hydrogen atoms are omitted for the sake of clarity.

1−**3** has a stronger bonding to the Cu(I) ion with the decreased electron-donating character of the halide. The Cu−X lengths of **1**−**3** become shorter as the van der Waals radii of X decreases. In sharp contrast to **1**−**3**, the Cu−$N_{pyridyl}$ length (2.268(8) Å) is much shorter than the Cu−$N_{triazolyl}$ length (2.446(10) Å) in **4**, revealing a stronger bonding of the Cu(I) atom to the N atom of the pyridyl, which is due to the introduction of the electron-donating methyl group. Compared with **1**−**3**, both Cu−N distances are markedly elongated and the N1−Cu−N4 angle is obviously enlarged for **4**, as a result of the increased steric congestion by the methyl substituent.

For $[Cu(N^{\wedge}N)(P_2)](ClO_4)$ complexes **5**, **6**, and **8**, the Cu(I) atom is located in an N_2P_2 distorted tetrahedral environment, in which bptzH or fptzH serves as a neutral chelating ligand. Analogous to **1**−**3**, complexes **5** and **6** have two distinctive Cu−N bonds with the Cu−$N_{triazolyl}$ distances (2.095(4) Å for **5**

dx.doi.org/10.1021/ic4002829 | Inorg. Chem. XXXX, XXX, XXX−XXX

Table 1. Crystal Data and Structure Refinement for the Halide Compounds 1−4

compound	1	2	3	4
formula	$C_{29}H_{29}ICuN_4P$	$C_{29}H_{29}BrCuN_4P$	$C_{29}H_{29}ClCuN_4P$	$C_{30}H_{31}ICuN_4P$
fw	654.97	607.98	563.52	669.00
T [K]	296(2)	296(2)	296(2)	296(2)
crystal system	monoclinic	monoclinic	monoclinic	monoclinic
space group	*Cc*	*Cc*	*Cc*	*Cc*
a [Å]	10.8694(2)	10.69550(10)	10.5931(4)	10.7879(10)
b [Å]	17.0146(3)	16.9158(2)	16.8769(6)	17.1097(17)
c [Å]	16.0390(3)	15.7249(2)	15.5198(6)	16.297(2)
α [deg]	90	90	90	90
β [deg]	99.9750(10)	97.9500(10)	97.240(2)	98.3540(10)
γ [deg]	90	90	90	90
V [Å^3]	2921.39(9)	2817.65(6)	2752.49(18)	2976.1(5)
Z	4	4	4	4
ρ_{calcd} [mg m^{-3}]	1.489	1.433	1.360	1.493
μ [mm^{-1}]	1.883	2.274	0.973	1.850
no. reflections collected	13648	10550	10582	6466
no. unique reflections	6041	4854	4212	3306
R_{int}	0.0183	0.0360	0.0471	0.0356
no. observed reflections	6041	4854	4212	3306
no. parameters	325	325	325	334
goodness of fit (GOF) on F^2	1.023	0.889	0.979	1.040
$R1$ ($I > 2\sigma(I)$)	0.0214	0.0326	0.0426	0.0515
$wR2$	0.0490	0.0654	0.0563	0.1300

Table 2. Crystal Data and Structure Refinement for Compounds 5−8

compound	5	6	7	8
formula	$C_{47}H_{44}ClCuN_4O_4P_2$	$C_{132}H_{105}Cl_3Cu_3F_9N_{12}O_{12}P_6{\cdot}3CHCl_3$	$C_{44}H_{34}CuF_3N_4P_2$	$C_{37}H_{38}ClCuN_4O_4P_2$
fw	889.79	3063.17	801.23	763.64
T [K]	296(2)	153(2)	296(2)	296(2)
crystal system	monoclinic	triclinic	monoclinic	monoclinic
space group	*C*2/*c*	$P\bar{1}$	$P2_1/n$	$P2_1/n$
a [Å]	32.625(4)	15.6798(15)	13.0571(2)	12.1535(3)
b [Å]	15.5875(19)	16.7611(16)	21.9601(3)	15.9763(3)
c [Å]	21.406(2)	27.175(3)	14.3551(2)	19.9227(4)
α [deg]	90	85.433(2)	90	90
β [deg]	124.976(2)	84.598(3)	106.3010(10)	106.2740(10)
γ [deg]	90	74.193(2)	90	90
V [Å^3]	8919.7(18)	6830.3(11)	3950.65(10)	3713.35(14)
Z	8	2	4	4
ρ_{calcd} [mg m^{-3}]	1.325	1.489	1.347	1.366
μ [mm^{-1}]	0.669	0.845	0.684	0.790
no. reflections collected	31492	79940	15839	29489
no. unique reflections	11090	30856	9096	8487
R_{int}	0.0928	0.0284	0.0377	0.0329
no. observed reflections	11090	30856	9096	8487
no. parameters	548	1820	487	442
goodness of fit (GOF) on F^2	0.968	1.066	1.007	1.031
$R1$ ($I > 2\sigma(I)$)	0.0698	0.0450	0.0496	0.0429
$wR2$	0.1620	0.1248	0.1166	0.1099

and avg. 2.0994(17) Å for **6**) being shorter than the Cu−$N_{pyridyl}$ distances (2.177(4) Å for **5** and avg. 2.1319(16) Å for **6**). Because of the steric effect of dppe in **8**, an unfavorable repulsion between the Cu(I) center and one adjacent methyl group of the *tert*-butyl substituent appears, as supported by the splitting behavior of the methylene and *tert*-butyl signals in the ^{1}H NMR spectrum. As a result, the Cu−$N_{pyridyl}$ bond of **8** is obviously shorter (2.061(2) Å) than those of **5** (2.177(4) Å) and **6** (av. 2.1319(16) Å), although the Cu−$N_{triazolyl}$ and Cu−P distances are still within the normal range. The N−Cu−N angle of **8** is somewhat greater, 82.01(8)°, because of the reduced steric congestion of dppe relative to PPh_3.[21] The P−Cu−P angles vary dramatically from 125.41(5)° for **5** and avg. 126.80(2)° for **6** to 91.97(3)° for **8**. For neutral species **7**, the Cu(I) ion is also in an N_2P_2 distorted tetrahedral arrangement with the Cu−$N_{triazolyl}$ length (2.016(2) Å) being obviously shorter than the Cu−$N_{pyridyl}$ distance (2.207(2) Å). The Cu−$N_{triazolyl}$ length (2.016(2) Å) of **7** is much shorter than those (2.0751(18)−2.119(2) Å) of **1**−**3**, **5**, **6**, and **8**, indicative of the

dx.doi.org/10.1021/ic4002829 | Inorg. Chem. XXXX, XXX, XXX−XXX

Table 3. Selected Bond Lengths and Angles of Compounds 1−4

Bond Lengths [Å]				
	1	2	3	4
Cu1−N1	2.1818(19)	2.189(3)	2.195(4)	2.268(8)
Cu1−N4	2.0751(18)	2.082(3)	2.087(4)	2.446(10)
Cu1−P1	2.2047(6)	2.2022(11)	2.1978(14)	2.171(3)
Cu1−X1	2.5886(3)	2.4293(6)	2.2962(13)	2.2063(14)
Bond Angles [deg]				
	1	2	3	4
N1−Cu1−N4	79.59(7)	79.04(12)	78.19(16)	86.9(3)
N1−Cu1−X1	110.00(6)	109.23(9)	108.32(11)	111.3(2)
N1−Cu1−P1	109.57(5)	110.87(9)	111.16(11)	116.5(3)
N4−Cu1−P1	123.59(6)	123.34(9)	122.14(10)	130.1(2)
N4−Cu1−X1	110.48(6)	110.06(9)	110.64(10)	107.6(2)
P1−Cu1−X1	116.83(2)	117.26(3)	118.48(5)	103.55(9)

significant effect of the anionic 1,2,4-triazolate, resulting from the NH deprotonation.

Photophysical and Electrochemical Properties in Fluid Solution. The absorption and emission spectra of three free ligands (fptzH, bptzH, and bmptzH) and their respective Cu(I) complexes **1**−**9** were investigated in CH_2Cl_2 solution at ambient temperature. All pertinent photophysical data are summarized in Table 5. The free ligands display multiple absorption bands in the UV region (<310 nm), attributed to the ligand-centered $^1\pi-\pi^*$ transitions, showing a certain red-shifting (fptzH < bptzH < bmptzH) with the increased electron-donating ability of the substituents on 3-(2′-pyridyl)-1,2,4-triazole. As shown in Figure 4 and Table 5, complexes **1**−**9** exhibit several absorption peaks in the 230−330 nm region ($\varepsilon > 10^4$ M^{-1} cm^{-1}), because of the $^1\pi-\pi^*$ transitions of both N^N and phosphine ligands, which are slightly red-shifted, because of the more-extended π-conjugation, relative to the free ligands. Moreover, complex **8** exhibits a clear low-energy absorption band centered at ∼366 nm, despite only a relatively weak low-energy absorption shoulder or tail ($\varepsilon < 5500$ M^{-1} cm^{-1}) being observed in the range of 330−400 nm for **1**−**7** and **9**, suggesting that these weak low-energy absorptions appearing at 330−400 nm are affected more significantly by the phosphine ligand than the N^N chelate and halide ligands. As suggested by TD-DFT studies (vide infra), the lowest-lying transition of **1**−**9** are ascribed as Cu(3d) → N^N and phosphine → N^N charge transfer (^{1}MLCT/^{1}LLCT) transitions, mixed with some halide-to-ligand charge transfer (^{1}XLCT) character for **1**−**4** and a small amount of intraligand (^{1}IL) charge transition inside the anionic fptz chelate for **7**.

In degassed CH_2Cl_2 solution at ambient temperature, complexes **5**−**9** show a broad single emission band (Figure 5) centered at 504, 547, 529, 581, and 525 nm with moderate quantum yields of 0.097, 0.048, 0.027, 0.016, and 0.140, respectively. The emission intensity is drastically quenched by oxygen in aerated solution. This, together with the emission lifetime (from several to a dozen microseconds), indicates that the emission may be phosphorescent in origin. However, any detectable solution emission is unobserved for the halide complexes **1**−**4** at room temperature, most likely as a result of fast structural relaxation occurring in the low-viscosity solution, as supported by the fact that complexes **1**−**4** display strong solid-state emissions (Table 5) due to the retardation of structural relaxation in the solid state. Hence, the rigidochromism, which has been reported for other photoactive transition-metal complexes,[22] appears for Cu(I) halide complexes **1**−**4**.

For complexes **5**, **8**, and **9** involving the same bptzH and different phosphine ligands, the emission peak shifts toward lower energy with $\lambda_{max} \approx 504$ nm for **5**, 525 nm for **9**, and 581 nm for **8**. The emission energy trend in fluid solutions of **5**, **9**, and **8** is largely in accord with that of their weak low-energy absorptions mentioned above, suggesting that both may originate from the same electronic excited states markedly affected by the phosphine ligand. The tendency of the emission peaks for **5**, **9**, and **8** is consistent with those for the $[Cu(phen)(P_2)]^+$, $[Cu(dmp)(P_2)]^+$, and $[Cu(ppb)(P_2)]^+$ systems (phen = 1,10-phenanthroline, dmp = 2,9-dimethyl-1,10-phenanthroline, ppb = 2-(2-pyridylbenzimidazolyl)-benzene; P_2 = 2PPh_3, DPEphos, and dppe).[21a,23] The sequence of the emission energy is contrary to the electron-donating ability of the phosphine ligands (PPh_3 < DPEphos < dppe).[24] Besides, it has been reported that a larger P−Cu−P angle can reduce the dσ^* interactions and increase the energy required for MLCT.[23] Thus, it is likely that the P−Cu−P angle plays a partial role on the emission variation of **5**, **9**, and **8**, and virtually the P−Cu−P angle of **5** (125.41°), **9** (110−120° in Cu(I) complexes),[23,25] and **8** (91.97°) follows the reverse order of the

Table 4. Selected Bond Lengths and Angles of Compounds 5−8

Bond Lengths [Å]				
	5	6[a]	7	8
Cu1−N1 (Cu2−N5, Cu3−N9)[a]	2.177(4)	2.1405(16), 2.1275(16), 2.1276(16)	2.207(2)	2.061(2)
Cu1−N4 (Cu2−N8, Cu3−N12)[a] (Cu1−N2)	2.095(4)	2.1001(17), 2.0934(17), 2.1046(17)	2.016(2)	2.119(2)
Cu1−P1 (Cu2−P3, Cu3−P5)[a]	2.2677(14)	2.2731(5), 2.2436(5), 2.2472(5)	2.2666(8)	2.2586(8)
Cu1−P2 (Cu2−P4, Cu3−P6)[a]	2.2776(15)	2.2357(5), 2.2581(5), 2.2705(6)	2.2578(8)	2.2781(8)
Bond Angles [deg]				
	5	6[a]	7	8
N1−Cu1−N4 (N5−Cu2−N8, N9−Cu3−N12)[a] (N1−Cu1−N2)	79.87(15)	79.36(6), 79.70(6), 79.33(6)	79.13(9)	82.01(8)
N1−Cu1−P1 (N5−Cu2−P3, N9−Cu3−P5)[a]	105.88(11)	98.06(4), 114.60(5), 115.65(5)	108.63(7)	129.60(6)
N1−Cu1−P2 (N5−Cu2−P4, N9−Cu3−P6)[a]	104.64(11)	117.60(4), 102.57(5), 106.32(5)	100.39(7)	119.23(6)
N4−Cu1−P1 (N8−Cu2−P3, N12−Cu3−P5)[a] (N2−Cu1−P1)	112.54(10)	103.48(5), 111.18(5), 109.29(5)	113.00(8)	115.32(6)
N4−Cu1−P2 (N8−Cu2−P4, N12−Cu3−P6)[a] (N2−Cu1−P2)	116.63(11)	116.29(5), 115.75(5), 109.52(5)	117.36(8)	122.31(6)
P1−Cu1−P2 (P3−Cu2−P4, P5−Cu3−P6)[a]	125.41(5)	129.81(2), 123.93(2), 126.67(2)	125.37(3)	91.97(3)

[a]There are three independent molecules in the asymmetric unit of complex **6**.

dx.doi.org/10.1021/ic4002829 | Inorg. Chem. XXXX, XXX, XXX−XXX

Table 5. Photophysical and Electrochemical Data of Pyridyl Triazole Ligands and Their Compounds 1−9

compound	medium	λ_{abs} [nm] (ε [M^{-1} cm^{-1}])[a]	λ_{em} [nm]	τ [μs]	Φ_{em} [%]	E_{ox} [V][b]
bmptzH	CH_2Cl_2	247 (17300), 284 (19660), 294 (15140)	343			
bptzH	CH_2Cl_2	248 (15910), 280 (15640), 290sh (11590)	322			
fptzH	CH_2Cl_2	238 (20890), 278 (14840), 285 (11820)	432			
1	CH_2Cl_2	274 (22620), 309 (8010), 353 (2100)				0.56
	solid		547 (590)[c]	21.7 (98)[c]	17.1	
2	CH_2Cl_2	274 (20730), 360 (1825)				0.61
	solid		551	18.2	47.6	
3	CH_2Cl_2	274 (20980), 316 (5620), 361 (1160)				0.61
	solid		571	20.5	17.2	
4	CH_2Cl_2	279 (21290), 364 (1220)				0.55
	solid		499	18.0	35.3	
5	CH_2Cl_2	265 (40930), 341 (3780)	504	12.0	9.7	1.45
	solid		456	107	41.8	
6	CH_2Cl_2	258 (41510), 343 (3930)	547	7.9	4.8	1.61
	solid		472 (536)[c]	20.2 (163)[c]	67.1	
7	CH_2Cl_2	249 (44550), 345 (1500)	529	6.9	2.7	1.58
	solid		496 (500)[c]	30.3 (95)[c]	53.3	
8	CH_2Cl_2	274 (34670), 366 (4660)	581	7.8	1.6	1.27
	solid		525	15.9	49.1	
9	CH_2Cl_2	272 (36930), 348 (5170)	525	15.0	14.0	1.37
	solid		468	26.9	40.4	

[a]Values shown in parentheses in this column represent the absorption peak data. [b]Potentials were quoted versus the ferrocenium/ferrocene reference ($Fc^{+/0}$ = 0.51 V); oxidation potentials were measured in dry DMF (for **1**−**4**) and CH_2Cl_2 (for **5**−**9**). [c]Value shown in parentheses represents data measured in the solid state at 77 K.

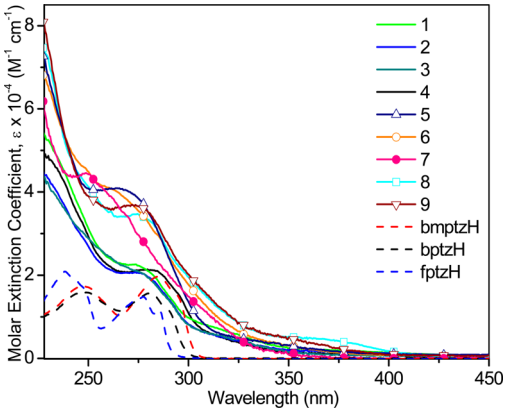

Figure 4. Absorption spectra of three free ligands and their respective complexes **1**−**9** in diluted CH_2Cl_2 solution at ambient temperature.

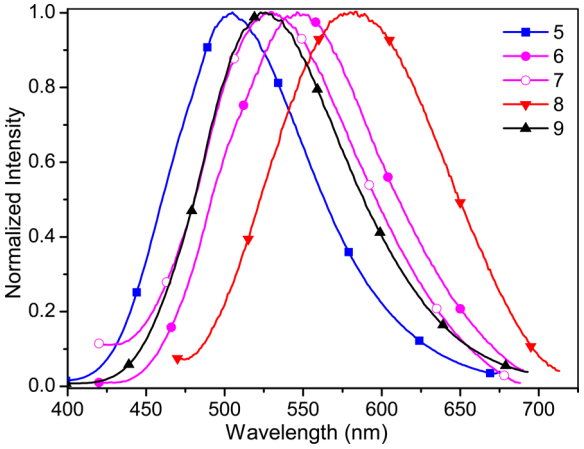

Figure 5. Emission spectra of complexes **5**−**9** in CH_2Cl_2 solution at ambient temperature.

emission maximum. Therefore, the emissions of **5**, **9**, and **8** are markedly affected by both the electronic properties of the phosphines and the P−Cu−P angles.[21a] Complex **6** shows a single, broad emission band at 547 nm with a 43 nm (1560 cm^{-1}) red-shift, relative to that of **5** (504 nm), as a consequence of the replacement of *tert*-butyl by electron-withdrawing trifluoromethyl on the 1,2,4-triazolyl, which lowers the energy level of the LUMO of **6** and thus reduces HOMO−LUMO gap. Complex **7** shows a broad emission at 529 nm with 18 nm (622 cm^{-1}) of blue-shift, compared with cationic complex **6**. This is perhaps due to NH deprotonation of the fptzH, in which the negative charge significantly raises the LUMO level and slightly influences the HOMO level, leading

dx.doi.org/10.1021/ic4002829 | Inorg. Chem. XXXX, XXX, XXX−XXX

to a larger HOMO−LUMO gap and thus a higher energy of emission.

The electrochemical behavior of the 1,2,4-triazole-based Cu(I) complexes has been investigated by cyclic voltammetry in dry DMF (for **1**−**4**) and CH_2Cl_2 (for **5**−**9**) using ferrocene as the internal standard, and the electrochemical data are presented in Table 5. During the anodic scan in DMF solution, halide complexes **1**−**4** display an irreversible oxidation peak with E_{pa} values of ∼0.56, 0.61, 0.61, and 0.55 V, respectively, ascribed to the oxidation of Cu(I) to Cu(II). For **5**−**9**, an irreversible oxidation peak is also observed in CH_2Cl_2 solution with E_{pa} values of ∼1.45, 1.61, 1.58, 1.27, and 1.37 V, respectively. It is noted that the oxidation potentials of **5**−**9** are much higher than those of **1**−**4**, which is mainly due to the replacement of the electron-donating halide by the good π-acceptor phosphine, which markedly decreases the electron density on the copper center, thus stabilizing the HOMO level. The oxidation potential sequence is **5** (1.45 V) > **9** (1.37 V) > **8** (1.27 V), which is contrary to the electron-donating ability of the phosphine ligands (PPh_3 < DPEphos < dppe), which implies that the HOMO orbital involves the contributions from the phosphine ligand. Moreover, the oxidation potentials of **5**−**7** appear to show that the HOMO level is also affected by the electronic nature of the N^N chelate.

Luminescence Properties in Solid State. The solid-state emission spectra of complexes **1**−**9** at ambient temperature and three representative complexes **1**, **6**, and **7** at 77 K were measured using powder samples (see Figures 6−9), and

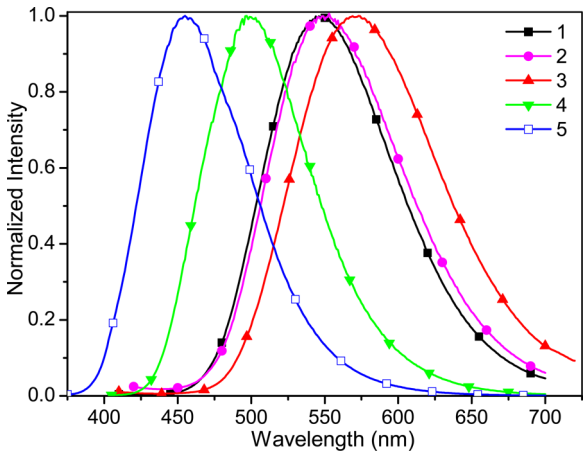

Figure 6. Emission spectra of complexes **1**−**5** in the solid state at ambient temperature.

relevant luminescence data are listed in Table 5. It is found that these Cu(I) complexes (**1**−**9**) are highly emissive in the solid state at ambient temperature. Halide complexes **1**−**3** with bptzH show an emission band centered at 547, 551, and 571 nm with the quantum yields of 0.171, 0.476, and 0.172, respectively. The emission maxima (λ_{max}) show the order of **1** < **2** < **3**, implying that the luminescence is influenced by the ligand-field strength of the halide (I^- < Br^- < Cl^-).[11] It is thus believed that the electronic nature of the emissive excited states of **1**−**3** is affected to some degree by $X^- \rightarrow \pi^*$(N^N) charge-transfer transitions. It is noted that the emission of **3** exhibits a 20 nm (636 cm^{-1}) red-shift, whereas that of **1** exhibits only a 4 nm (133 cm^{-1}) blue-shift, compared to that of **2**, suggesting that the emission is also affected by the electron-donating nature of the halide (I^- > Br^- > Cl^-), thus influencing the

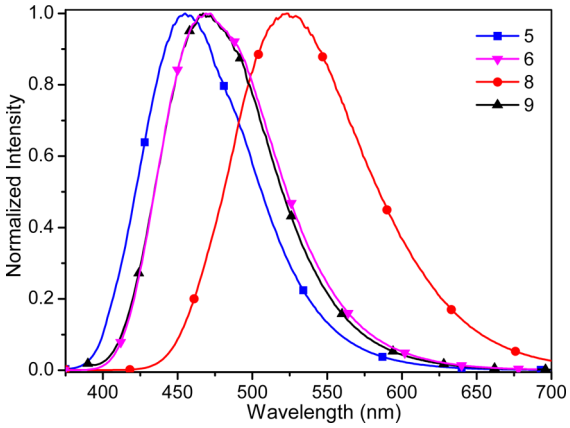

Figure 7. Emission spectra of complexes **5**, **6**, **8**, and **9** in the solid state at ambient temperature.

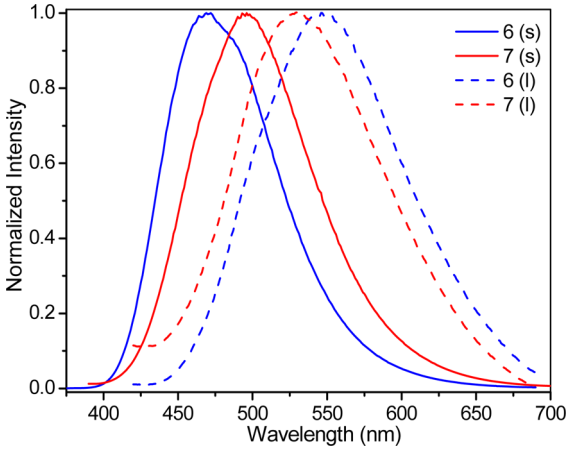

Figure 8. Emission spectra of complexes **6** and **7** in CH_2Cl_2 solution (dashed lines) and in the solid state (solid lines) at ambient temperature.

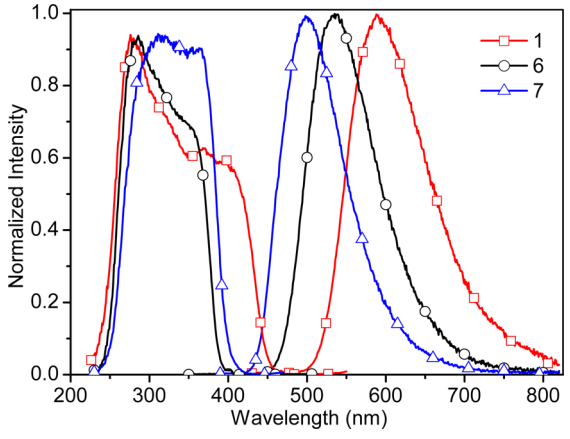

Figure 9. Excitation and emission spectra of complexes **1**, **6**, and **7** in the solid state at 77 K.

HOMO level localized at the Cu(I) center. Complex **4** gives a solid-state emission with the maximum at 499 nm and a good quantum yield of 0.353 with remarkable blue-shift (∼48 nm, 1759 cm^{-1}), relative to that of **1** (547 nm). The blue-shift may be due to the introduction of the electron-donating methyl on the 2-pyridyl of **1**, which raises the LUMO level, thus increases the HOMO−LUMO gap.

dx.doi.org/10.1021/ic4002829 | Inorg. Chem. XXXX, XXX, XXX−XXX

Table 6. Absorption and Emission Transitions for 1−8 in CH_2Cl_2 Solution Calculated by TD-DFT Method at the PBE1PBE Level

complex	state	transition (CI coef.)	E [nm] (eV)	O.S.	assignment	measured value [nm]
1	S_1	HOMO→LUMO (0.6849)	376.62 (3.29)	0.0236	^{1}MLCT/^{1}XLCT/^{1}LLCT	353
2	S_1	HOMO→LUMO (0.6804)	381.48 (3.25)	0.0274	^{1}MLCT/^{1}XLCT/^{1}LLCT	360
3	S_1	HOMO→LUMO (0.6789)	390.56 (3.17)	0.0328	^{1}MLCT/^{1}XLCT/^{1}LLCT	361
4	S_1	HOMO→LUMO (0.6959)	369.43 (3.36)	0.0327	^{1}MLCT/^{1}XLCT/^{1}LLCT	364
5	T_1	HOMO-2→LUMO (0.7890)	556.53 (2.23)	0.0000	^{3}IL	504
	S_1	HOMO→LUMO (0.6914)	328.65 (3.77)	0.0516	^{1}MLCT/^{1}LLCT	341
6	T_1	HOMO→LUMO (0.6912)	577.23 (2.15)	0.0000	^{3}IL/^{3}MLCT/^{3}LLCT	547
	S_1	HOMO→LUMO (0.6937)	341.30 (3.63)	0.0488	^{1}MLCT/^{1}LLCT	343
7	T_1	HOMO→LUMO (0.5750) HOMO-1→LUMO (−0.5125)	516.76 (2.40)	0.0000	^{3}IL/^{3}MLCT/^{3}LLCT	529
	S_1	HOMO-1→LUMO (0.4883) HOMO→LUMO (0.3833) HOMO-3→LUMO (0.2216) HOMO-2→LUMO (0.2179)	318.07 (3.90)	0.0257	^{1}MLCT/^{1}LLCT/^{1}IL	345
8	T_1	HOMO→LUMO (0.7062)	691.25 (1.79)	0.0000	^{3}IL/^{3}MLCT/^{3}LLCT	581
	S_1	HOMO→LUMO (0.6934)	359.61 (3.45)	0.0625	^{1}MLCT/^{1}LLCT	366

dx.doi.org/10.1021/ic4002829 | Inorg. Chem. XXXX, XXX, XXX−XXX

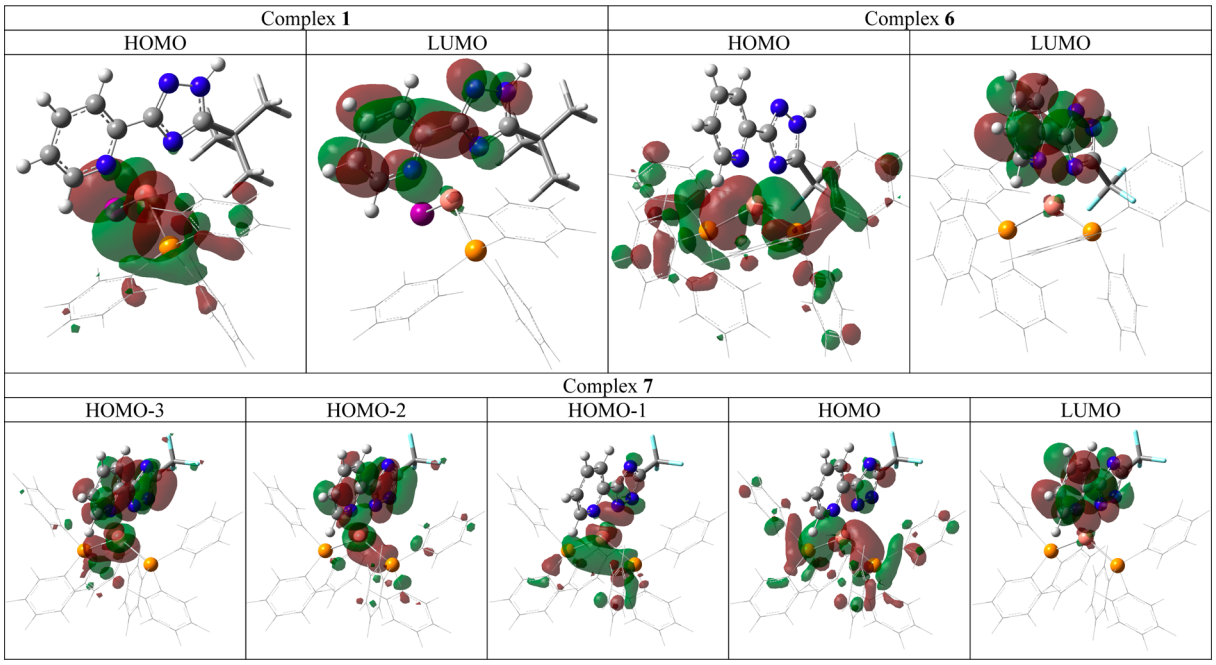

Figure 10. Plots of frontier orbitals involved in the lowest-lying electronic absorption transitions of complexes **1**, **6**, and **7**.

Similarly, complexes **5**−**9** in solid-state show a broad and unstructured emission profile with maxima at 456, 472, 496, 525, and 468 nm and quantum yields of 0.418, 0.671, 0.533, 0.491, and 0.404, respectively. The emission maxima, to some extent, are blue-shifted, relative to their corresponding solutions, as a result of the rigid medium. Moreover, the solid emission maxima of **5**, **9**, and **8** are in agreement with those in solution (**5** < **9** < **8**). The solid emission of **6** (472 nm) is red-shifted by 16 nm (743 cm^{-1}), relative to that of **5** (456 nm), because of the substitution of the *tert*-butyl group by a trifluoromethyl group. Interestingly, the solid emission of **7** shows a 24 nm (1025 cm^{-1}) red-shift, whereas the solution emission exhibits an 18 nm (622 cm^{-1}) blue-shift, relative to that of **6**. Such an anomaly can be rationalized in terms of a less rigid molecular structure of **7** than that of **6** upon the ring inversion of the 1,2,4-triazolyl mediated by NH deprotonation, under a basic medium.

Upon cooling to 77 K, the emission spectra (λ_{max}) for three representative complexes—**1** (590 nm), **6** (536 nm), and **7** (500 nm)—exhibit a bathochromic shift of 4−64 nm (161−2530 cm^{-1}), relative to those at ambient temperature, along with a marked increase in emission lifetime (95−163 μs). Such a luminescence behavior is frequently observed for emissive Cu(I) complexes with small singlet−triplet energy gaps $\Delta E(S_1-T_1)$ and is generally assigned to a decrease in thermally activated delayed fluorescence (TADF).[8d,10,13e,18k,26] At low temperatures, thermally activated population of the higher-lying state with faster radiative rate is suppressed, resulting in a red-shifted emission and a longer excited-state lifetime. Moreover, the solid emission peak of **6** (472 nm) at room temperature is remarkably blue-shifted, with respect to that (536 nm) measured at 77 K, whereas the solid emission profile of **7** at ambient temperature resembles that recorded at 77 K, indicating that the ring inversion and NH deprotonation of the 1,2,4-triazolyl have a significant impact on the emissive properties.

Theoretical Investigations. To gain insight into the photophysical properties of the 1,2,4-triazole-based Cu(I) complexes, the time-dependent density functional theory (TD-DFT)[27]/PBE1PBE[28] calculations were performed. The calculated lowest-lying absorptions of **1**−**8** and emission transition properties of **5**−**8** in CH_2Cl_2 media are summarized in Table 6. The frontier molecular orbitals involved in the lowest-lying electronic absorption transitions of **1**, **6**, and **7** are depicted in Figure 10. More figures and tables on TD-DFT studies of **1**−**8** are provided in the Supporting Information (see Tables S1−S10 and Figures S6−S25).

As shown in Figure 10, Table 6, and Table S1 in the Supporting Information, the HOMO of **1**, as an example of the halide complexes **1**−**4**, has contributions from Cu(3d) (42.86%), PPh_3 (26.95%), and I (26.76%), while the LUMO is basically localized on bptzH (96.58%). Hence, the calculated lowest-energy absorption at 377 nm from HOMO → LUMO transition is attributable to the ^{1}MLCT/^{1}XLCT/^{1}LLCT (Cu(3d)/I/PPh_3 → bptzH) state, which is in reasonable agreement with the experimentally measured one at 353 nm. The calculated lowest-energy absorption wavelengths follow a ranking of

4 (369 nm) < **1** (377 nm) < **2** (381 nm) < **3** (391 nm)

(see Table 6), which agrees with that of the measured emission

4 (499 nm) < **1** (547 nm) < **2** (551 nm) < **3** (571 nm)

(see Table 5). As an example of cationic complexes **5**, **6**, and **8**, the HOMO of **6** is primarily composed of Cu(3d) (31.05%) and two PPh_3 (66.46%), while the LUMO is essentially centered on fptzH (94.60%) (see Table S6 in the Supporting Information). Thus, the calculated lowest-lying absorption of **6** is assigned to a mixed ^{1}MLCT/^{1}LLCT (Cu(3d)/PPh_3 → fptzH) character. However, for **7** bearing deprotonated fptz, the LUMO is predominantly located on the anionic fptz, whereas the HOMO, HOMO-1, HOMO-2, and HOMO-3 are almost resident on Cu(3d), PPh_3, and fptz (see Table S7 in the Supporting Information). Hence, its calculated lowest-energy absorption at 318 nm is typical of a significant ^{1}MLCT (Cu(3d) → fptz) character mixed with a certain degree of the

dx.doi.org/10.1021/ic4002829 | Inorg. Chem. XXXX, XXX, XXX−XXX

^{1}LLCT transition ($PPh_3 \rightarrow$ fptz) and the intraligand (^{1}IL) transition inside fptz.

The emissive properties of **5**–**8** in CH_2Cl_2 media were investigated by TD-DFT/PBE1PBE calculations, according to the optimized lowest triplet excited-state T_1 geometries. As depicted in Table 6, as well as Table S9 and Figures S16–S20 in the Supporting Information, the triplet emissive states of **6** and **8** corresponding to the HOMO→LUMO transitions are attributed to the ^{3}MLCT transitions mixed with some ^{3}LLCT/^{3}IL characters, while the triplet excited state of **7** from the HOMO → LUMO and HOMO-1 → LUMO transitions can be assigned as a mixed ^{3}MLCT/^{3}LLCT/^{3}IL character. However, despite the fact that the lowest singlet (S_1) absorption of **5** has a substantial ^{1}MLCT transition (see Table S5 in the Supporting Information), its lowest triplet-state (T_1) is identified as the ^{3}IL transition inside bptzH. Such a phenomenon can be rationalized via a larger difference between the ^{3}IL level and the ^{3}MLCT/^{3}LLCT levels of **5**, relative to those of **6**–**8**, which leads to a relatively complete energy transfer from the higher ^{3}MLCT/^{3}LLCT level to the lower ^{3}IL level for **5**.

The solid emission properties of **1** and **4**–**6** were also calculated using the TD-DFT/PBE1PBE method, based on their single-crystal structures (see Table S10 and Figures S21–S25 in the Supporting Information). The lowest triplet excited state of **1** in the solid state is assigned as the ^{3}MLCT/^{3}XLCT characters, while the solid-state emission of **4** is attributable to the ^{3}(MLCT/LLCT/XLCT) transitions. The calculated HOMO–LUMO gaps are **1** (3.33 eV) < **4** (3.42 eV), which is consistent with that of the measured solid emission energies. For **5**, the calculated solid emission displays mixed transition properties of ^{3}IL/^{3}LLCT/^{3}MLCT, which is distinctly different from that (^{3}IL) of its calculated solution emission. This may be due to the effect of the rigid medium retarding the structural relaxation being favorable to the energy transfer from ^{3}MLCT/^{3}LLCT state to ^{3}IL state for **5** in solution. The calculated solid emission of **6** is assigned as a mixed ^{3}(MLCT/LLCT) character. The calculated HOMO–LUMO gaps follow **5** (4.55 eV) > **6** (3.84 eV), which is in reasonable agreement with that of the experimentally measured solid emissions of **5** (456 nm) and **6** (472 nm).

CONCLUSIONS

We have designed and synthesized a new series of luminescent monometallic Cu(I) complexes with functionalized 3-(2′-pyridyl)-1,2,4-triazole ligands. Their structural features and photophysical properties have been fully investigated. These 1,2,4-triazole-based Cu(I) complexes **1**–**9** are fairly air-stable both in solution and in the solid state. They show a relatively weak low-energy absorption in CH_2Cl_2 solution, ascribed to the charge-transfer transitions with appreciable MLCT character as supported by TD-DFT calculations. Complexes **5**–**9** have a good luminescence properties in degassed CH_2Cl_2 solution, despite the halide complexes **1**–**4** being nonemissive in fluid solution, In contrast, complexes **1**–**9** are all strongly emissive in the solid state at ambient temperature, and the emissive properties are well-modulated via the structural modification of 3-(2′-pyridyl)-1,2,4-triazole and the change of the ancillary ligands such as phosphine and halide. The interconversion between cationic complex **6** and neutral derivative **7** has been successfully achieved through the ring inversion of the 1,2,4-triazolyl regulated by the controllable NH ↔ N$^-$ transformation, in which they exhibit distinct emission properties in both solution and solid states. The results presented herein might provide new insight into the synthesis of blue phosphorescent materials of the 3-(2′-pyridyl)-1,2,4-triazole-based copper(I) complexes with potentially high luminescence efficiency.

EXPERIMENTAL SECTION

General Procedures and Materials. All reactions were performed under a N_2 atmosphere, using anhydrous solvents or solvents treated with an appropriate drying reagent. Commercially available reagents were used without further purification unless otherwise stated. $[Cu(CH_3CN)_4](ClO_4)$[29] and $[Cu(PPh_3)_2(CH_3CN)_2](ClO_4)$[30] were prepared according to the literature methods. The functionalized 3-(2′-pyridyl)-1,2,4-triazole ligands including 5-trifluoromethyl-3-(2-pyridyl)-1,2,4-triazole (fptzH), 5-*tert*-butyl-3-(2-pyridyl)-1H-1,2,4-triazole (bptzH), and 5-*tert*-butyl-3-(6-methyl-2-pyridyl)-1H-1,2,4-triazole (bmptzH) were synthesized using previously reported procedures.[31]

Caution! *The perchlorate salts are potentially explosive and should be handled carefully in small amounts.*

Preparation of Cu(bptzH)(PPh$_3$)I (1). A mixture of CuI (36.2 mg, 0.190 mmol) and PPh_3 (100.2 mg, 0.382 mmol) was stirred in CH_2Cl_2 (ca. 15 mL) for 30 min at ambient temperature to give a colorless solution. A solution of bptzH (38.7 mg, 0.191 mmol) in CH_2Cl_2 (ca. 6 mL) was added, and the mixture was stirred for 3 h, affording a yellow precipitate. The precipitate (**1**, 109.5 mg, 0.167 mmol, 88%) was collected by filtration, washed with CH_2Cl_2 and diethyl ether, and dried under vacuum. X-ray-quality yellow crystals were grown via the slow diffusion of methanol into the DMF solution of **1** after 4 days. ESI-MS: m/z 527 $[M-I]^+$. ^{1}H NMR (DMSO-d_6, 400 MHz): δ 14.49 (s, 1H), 8.38 (s, 1H), 8.19 (d, 1H, J = 7.6 Hz), 8.05 (t, 1H, J = 6.4 Hz), 7.65–7.60 (m, 3H), 7.58–7.53 (m, 3H), 7.40–7.38 (m, 10H), 1.31 (s, 9H). ^{31}P{^{1}H} NMR (DMSO-d_6, 202.3 MHz): δ −6.05 (s, PPh$_3$). Anal. Calcd for $C_{29}H_{29}ICuN_4P$: C, 53.18; H, 4.46; N, 8.55. Found: C, 53.32; H, 4.58; N, 8.43.

Preparation of Cu(bptzH)(PPh$_3$)Br (2). Complex **2** was prepared following the procedure for **1**, using CuBr (32.6 mg, 0.227 mmol), PPh_3 (119.3 mg, 0.455 mmol), and bptzH (46.1 mg, 0.228 mmol), which resulted in the formation of a light yellow precipitate (**2**, 112.3 mg, 0.185 mmol, 81%). Light yellow crystals were afforded via the slow diffusion of diethyl ether into the DMF solution of **2** after 3 days. ESI-MS: m/z 527 $[M-Br]^+$. ^{1}H NMR (DMSO-d_6, 400 MHz): δ 14.45 (s, 1H), 8.35 (s, 1H), 8.19 (s, 1H), 8.05 (s, 2H), 7.65–7.60 (m, 1H), 7.58–7.54 (m, 2H), 7.45–7.37 (m, 12H), 1.31 (s, 9H). ^{31}P{^{1}H} NMR (DMSO-d_6, 202.3 MHz): δ −5.23 (s, PPh$_3$). Anal. Calcd for $C_{29}H_{29}BrCuN_4P$: C, 57.29; H, 4.81; N, 9.22. Found: C, 57.13; H, 4.75; N, 9.33.

Preparation of Cu(bptzH)(PPh$_3$)Cl (3). Complex **3** was prepared following the procedure for **1**, using CuCl (29.3 mg, 0.296 mmol), PPh_3 (155.4 mg, 0.592 mmol), and bptzH (60.0 mg, 0.297 mmol), which led to the formation of a light yellow precipitate (**3**, 130.2 mg, 0.231 mmol, 78%). Light yellow crystals were obtained by slow diffusion of diethyl ether into the DMF solution of **3** after 3 days. ESI-MS: m/z 527 $[M-Cl]^+$. ^{1}H NMR (DMSO-d_6, 400 MHz): δ 14.39 (s, 1H), 8.30 (s, 1H), 8.16 (d, 1H, J = 7.6 Hz), 8.00 (t, 1H, J = 7.4 Hz), 7.65–7.56 (m, 1H), 7.45–7.32 (m, 15H), 1.29 (s, 9H). ^{31}P{^{1}H} NMR (DMSO-d_6, 202.3 MHz): δ −4.69 (s, PPh$_3$). Anal. Calcd

dx.doi.org/10.1021/ic4002829 | Inorg. Chem. XXXX, XXX, XXX–XXX

for $C_{29}H_{29}ClCuN_4P$: C, 61.81; H, 5.19; N, 9.94. Found: C, 61.94; H, 5.23; N, 9.89.

Preparation of Cu(bmptzH)(PPh$_3$)I (4). Complex **4** was prepared following the procedure for **1**, using CuI (38.1 mg, 0.200 mmol), PPh_3 (105.3 mg, 0.401 mmol), and bmptzH (43.5 mg, 0.201 mmol), which resulted in the generation of a light yellow precipitate (**4**, 101.7 mg, 0.152 mmol, 76%). Light yellow crystals were grown by slow diffusion of diethyl ether into the DMF solution of **4** after 3 days. ESI-MS: m/z 541 $[M-I]^+$. ^{1}H NMR (DMSO-d_6, 400 MHz): δ 14.48 (s, 1H), 8.05−7.96 (m, 2H), 7.65−7.53 (m, 3H), 7.44−7.33 (m, 13H), 2.34 (s, 3H), 1.24 (s, 9H). ^{31}P{^{1}H} NMR (DMSO-d_6, 202.3 MHz): δ −7.91 (s, PPh$_3$). Anal. Calcd for $C_{30}H_{31}ICuN_4P$: C, 53.86; H, 4.67; N, 8.37. Found: C, 53.95; H, 4.72; N, 8.41.

Preparation of [Cu(bptzH)(PPh$_3$)$_2$](ClO$_4$) (5). A CH_2Cl_2 solution (10 mL) of bptzH (18.6 mg, 0.092 mmol) and $[Cu(PPh_3)_2(CH_3CN)_2](ClO_4)$ (70.2 mg, 0.091 mmol) was stirred at ambient temperature for 4 h to give a light yellow solution. The solvent was then removed at reduced pressure. The resultant residue was again dissolved in a mixture of CH_2ClCH_2Cl/CH_2Cl_2 (1:5 v/v), and slow diffusion of petroleum ether into the above solution yielded creamy crystals of **5** (64.5 mg, 0.072 mmol, 79%). ESI-MS: m/z 790 $[M-ClO_4]^+$. ^{1}H NMR (DMSO-d_6, 400 MHz): δ 14.72 (s, 1H), 8.23 (d, 1H, J = 8.0 Hz), 8.04 (t, 1H, J = 7.6 Hz), 7.91 (s, 1H), 7.46 (t, 6H, J = 7.4 Hz), 7.41−7.33 (m, 13H), 7.13 (t, 12H, J = 8.0 Hz), 1.16 (s, 9H). ^{31}P{^{1}H} NMR (DMSO-d_6, 202.3 MHz): δ −0.19 (s, PPh$_3$). Anal. Calcd for $C_{47}H_{44}ClCuN_4O_4P_2$: C, 63.44; H, 4.98; N, 6.30. Found: C, 63.26; H, 4.74; N, 6.47.

Preparation of [Cu(fptzH)(PPh$_3$)$_2$](ClO$_4$) (6). Complex **6** was prepared following the procedure for **5**, using $[Cu(PPh_3)_2(CH_3CN)_2](ClO_4)$ (72.4 mg, 0.094 mmol) and fptzH (20.2 mg, 0.094 mmol). The resulting residue was again dissolved in CH_2Cl_2, and slow diffusion of petroleum ether into the above solution afforded light yellow crystals of **6** (69.6 mg, 0.077 mmol, 82%). ESI-MS: m/z 802 $[M-ClO_4]^+$. ^{1}H NMR (CD_2Cl_2, 400 MHz): δ 14.47 (s, 1H), 8.57 (d, 1H, J = 8.8 Hz), 8.10−8.08 (m, 2H), 7.45 (t, 7H, J = 6.8 Hz), 7.29 (t, 12H, J = 7.6 Hz), 7.18 (d, 12H, J = 7.2 Hz). ^{19}F{^{1}H} NMR (CD_2Cl_2, 376.5 MHz): δ −64.25 (s, CF_3). ^{31}P{^{1}H} NMR (DMSO-d_6, 202.3 MHz): δ −2.81 (s, PPh$_3$). Anal. Calcd for $C_{44}H_{35}ClCuF_3N_4O_4P_2$: C, 58.61; H, 3.91; N, 6.21. Found: C, 58.73; H, 4.12; N, 6.25.

Preparation of Cu(fptz)(PPh$_3$)$_2$ (7). A methanol solution (10 mL) of fptzH (25.8 mg, 0.121 mmol) and $[Cu(PPh_3)_2(CH_3CN)_2](ClO_4)$ (92.5 mg, 0.120 mmol) was stirred at room temperature for 2 h, generating a light yellow solution. Powdered NaOH (5.2 mg, 0.130 mmol) was added, and this admixture was stirred for another 3 h, yielding an almost colorless suspension. After the solvent was evaporated at reduced pressure, the solid residue was extracted with CH_2Cl_2. Subsequent diffusion of n-hexane into the CH_2Cl_2 solution gave nearly colorless crystals of **7** (75.2 mg, 0.094 mmol, 78%). ESI-MS: m/z 802 $[M+1]^+$. ^{1}H NMR (CD_2Cl_2, 400 MHz): δ 8.11 (d, 1H, J = 8.0 Hz), 7.91 (s, 1H), 7.79 (t, 1H, J = 6.8 Hz), 7.34−7.38 (m, 6H), 7.22 (d, 24H, J = 4.4 Hz), 7.06 (s, 1H). ^{19}F{^{1}H} NMR (CD_2Cl_2, 376.5 MHz): δ −63.29 (s, CF_3). ^{31}P{^{1}H} NMR (DMSO-d_6, 202.3 MHz): δ −1.11 (s, PPh$_3$). Anal. Calcd for $C_{44}H_{34}CuF_3N_4P_2$: C, 61.81; H, 5.19; N, 9.94. Found: C, 61.93; H, 5.26; N, 9.87.

Preparation of [Cu(bptzH)(dppe)](ClO$_4$) (8). A solution of $[Cu(CH_3CN)_4](ClO_4)$ (36.7 mg, 0.112 mmol) and 1,2-bis(diphenylphosphino)ethane (dppe) (44.8 mg, 0.112 mmol) in CH_2Cl_2 (8 mL) was stirred for 30 min at room temperature. A solution of bptzH (22.7 mg, 0.112 mmol) in CH_2Cl_2 (5 mL) was added, and this admixture was stirred for another 3 h to get a yellow solution. The solvent was evaporated to dryness at reduced pressure. The residue was dissolved in CH_2Cl_2, and a slow diffusion of diethyl ether into the above solution gave yellow crystals of **8** (75.3 mg, 0.099 mmol, 88%). ESI-MS: m/z 664 $[M-ClO_4]^+$. ^{1}H NMR (DMSO-d_6, 400 MHz): δ 14.81 (s, 1H), 8.42 (d, 1H, J = 8.0 Hz), 8.23 (t, 2H, J = 7.6 Hz), 7.63 (t, 1H, J = 6.2 Hz), 7.44−7.34 (m, 16H), 7.27−7.20 (m, 4H), 2.79 (s, 3H), 2.54 (s, 1H), 1.21 (s, 2H), 0.92 (s, 7H). ^{31}P{^{1}H} NMR (DMSO-d_6, 202.3 MHz): δ −7.41 (s, dppe). Anal. Calcd for $C_{37}H_{38}ClCuN_4O_4P_2$: C, 58.19; H, 5.02; N, 7.34. Found: C, 58.13; H, 4.95; N, 7.41.

Preparation of [Cu(bptzH)(DPEphos)](ClO$_4$) (9). A solution of $[Cu(CH_3CN)_4](ClO_4)$ (35.4 mg, 0.108 mmol) and bis[2-(diphenylphosphino)phenyl]ether (DPEphos) (58.3 mg, 0.108 mmol) in CH_2Cl_2 (10 mL) was stirred for 30 min at room temperature. A solution of bptzH (21.9 mg, 0.108 mmol) in CH_2Cl_2 (5 mL) was added, and this mixture was stirred for another 3 h to afford a nearly colorless solution. The solvent was evaporated to dryness at reduced pressure. The residue was dissolved in CH_2Cl_2, and slow diffusion of diethyl ether into the above solution gave white crystals of **9** (81.2 mg, 0.090 mmol, 83%). ESI-MS: m/z 804 $[M-ClO_4]^+$. ^{1}H NMR (DMSO-d_6, 400 MHz): δ 14.65 (s, 1H), 8.26 (d, 1H, J = 8.0 Hz), 8.07−8.00 (m, 2H), 7.47−7.25 (m, 18H), 7.13 (t, 5H, J = 7.6 Hz), 6.82−6.75 (m, 6H), 1.04 (s, 9H). ^{31}P{^{1}H} NMR (DMSO-d_6, 202.3 MHz): δ −13.53 (s, DPEphos). Anal. Calcd for $C_{47}H_{42}ClCuN_4O_5P_2$: C, 62.46; H, 4.68; N, 6.20. Found: C, 62.35; H, 4.57; N, 6.31.

Crystal Structural Determination. Data collections for compounds **1**−**8** were performed on a Bruker SMART Apex II CCD diffractometer using graphite-monochromated Mo Kα radiation (λ = 0.71073 Å). The datasets were corrected for Lorentz and polarization factors as well as for absorption by SADABS program. The structures were solved by direct methods and refined on F^2 by full-matrix least-squares methods using the SHELXTL-97 program package.[32] The heavy atoms were located from E-map, and other non-hydrogen atoms were found in subsequent difference Fourier syntheses. All non-hydrogen atoms were refined anisotropically, while the hydrogen atoms were generated geometrically with isotropic thermal parameters.

Physical Measurements. ^{1}H, ^{19}F{^{1}H}, and ^{31}P{^{1}H} NMR spectra were recorded on Bruker Avance III (400 MHz) spectrometer with $SiMe_4$ as the internal reference and 85% H_3PO_4 as the external reference. Elemental analyses (C, H, and N) were conducted on a Perkin−Elmer Model 240C elemental analyzer. UV−vis absorption spectra in CH_2Cl_2 solution were measured on a Shimadzu Model UV-2550 spectrometer. Electrospray ionization mass spectrometry (ESI-MS) was recorded on a Finnigan Model DECAX-30000 LCQ mass spectrometer, using DMF−methanol or dichloromethane−methanol as the mobile phase. The photoluminescence properties in CH_2Cl_2 solution and in the solid state were determined on an Edinburgh analytical instrument (Model F900 fluorescence spectrometer) with a thermoelectrically cooled Hamamatsu Model R3809 photomultiplier tube. The emission quantum yields (Φ_{em}) of **5**−**9** in CH_2Cl_2 solution at room temperature were calculated by $\Phi_s = \Phi_r(B_r/B_s)(n_r/n_s)^2(D_s/D_r)$ using fluorescein in H_2O as the standard (Φ_{em} = 0.79), where the subscripts "r" and "s" denote reference

dx.doi.org/10.1021/ic4002829 | Inorg. Chem. XXXX, XXX, XXX−XXX

standard and the sample solution, respectively, and n, D, and Φ are the refractive index of the solvents, the integrated intensity, and the luminescence quantum yield, respectively.[33] The quantity B is calculated by $B = 1-10^{-AL}$, where A is the absorbance at the excitation wavelength and L is the optical path length. An integrating sphere (Labsphere) was applied to measure the quantum yields of **1**−**9** in the solid state. The cyclic voltammogram were carried out in a Princeton Applied Research Model 263A potentiostat/galvanostat analyzer using a glassy carbon disk working electrode, a platinum counter electrode, and a Ag/AgCl reference electrode. All experiments were performed in dry DMF (for **1**−**4**) and CH_2Cl_2 (for **5**−**9**) solvents with 0.1 M tertrabutylammonium hexafluorophosphate as the supporting electrolyte. The potentials are quoted versus the ferrocenium/ferrocene couple ($Fc^{+/0}$ = 0.51 V).

Computational Methodology. All the calculations were carried out by using the Gaussian 03 program package[34] to get insight into the photophysical properties of these 1,2,4-triazole-based Cu(I) complexes **1**−**8**. First, the density functional theory (DFT)[35] at the gradient-corrected correlation functional PBE1PBE[28] and unrestricted PBE1PBE (UPBE1PBE) levels, respectively, was used to optimize the ground-state (S_0) geometries of complexes **1**−**8** and the triple excited-state (T_1) geometries of complexes **5**−**8** without symmetry constraint. The initial structures were extracted from the crystallographically determined geometries. During the optimization processes, the convergent values of maximum force, root-mean-square (RMS) force, maximum displacement, and RMS displacement are set by default. To analyze the spectroscopic properties, 60 singlet excited states for **1**−**8** and 6 triplet excited states for **5**−**8** in CH_2Cl_2 solution were calculated by the time-dependent DFT (TD-DFT)[27] method at the same functional used in the geometrical optimization, respectively, based on the optimized ground-state S_0 and lowest-energy triplet excited-state T_1 geometries. The solvent effects in CH_2Cl_2 media were taken into account by performing the self-consistent reaction field (SCRF) calculations using the polarizable continuum model method (PCM).[36] To analyze the emission properties in the solid states, the TD-DFT/PBE1PBE calculations were carried out on the model structures derived from the crystallographic data with all C−H bond length sets by 1.09 Å and N−H ones by 1.01 Å.[37] In these calculations, the Hay−Wadt double-ζ with a Los Alamos relativistic effect basis set (LANL2DZ)[38] consisting of the effective core potentials (ECP) was employed for the Cu, P, I, Br, and Cl atoms, and the 6-31G(p,d) basis set[39] was used for the remaining atoms. To precisely describe the molecular properties, one additional f-type polarization function was implemented for the Cu atom (α_f = 0.24), and a d-type polarization function was employed for the P (α_d = 0.34), I (α_d = 0.266), Br (α_d = 0.389), and Cl (α_d = 0.514) atoms.[40] Visualization of the optimized structures and frontier molecular orbitals were performed by GaussView. The Ros and Schuit method (C-squared population analysis method, SCPA)[41] is supported to analyze the partition orbital composition, using the Multiwfn 2.4 program.[42]

■ ASSOCIATED CONTENT

Supporting Information

Crystallographic data (CIF file) of **1**−**8**. Perspective drawings of **2**−**4** and the cations of **5** and **8**, tables and figures regarding the TD-DFT calculations of **1**−**8**, and characterization data of **1**−**9** (PDF file). This material is available free of charge via the Internet at http://pubs.acs.org.

■ AUTHOR INFORMATION

Corresponding Author

*E-mail: gzchenjinglin@126.com (J.-L.C.), jy_wang@fjirsm.ac.cn .

Notes

The authors declare no competing financial interest.

■ ACKNOWLEDGMENTS

We thank the financial support from the NSFC (Nos. 21163009, 21001057, and 21161008), the Key Project of Chinese Ministry of Education (No. 211088), the Advanced Program for the Retuned Overseas Chinese Scholars of MOHRSS (No. 474[2011]), the Training Program for Jiangxi Provincial Young Scientists (No. 20122BCB23016), the Key Project of Education Department of Jiangxi Province (No. GJJ13436), the Foundation of State Key Laboratory of Structural Chemistry (No. 20110015), and the Scientific Research Foundation of Jiangxi University of Science and Technology (No. JXXJ12072).

■ REFERENCES

(1) (a) Cotton, F. A.; Wilkinson, G. *Advanced Inorganic Chemistry*; Wiley: New York, 1980. (b) Kalyanasundaram, K. *Photochemistry of Polypyridine and Porphyrin Complexes*; Academic Press: London, 1992. (c) Vogler, A.; Kunkely, H. *Top. Curr. Chem.* **2001**, *213*, 143−182. (d) Balzani, V.; Campagna, C. *Photochemistry and Photophysics of Coordination Compounds I*; Springer: Berlin, 2007. (e) Balzani, V.; Campagna, C. *Photochemistry and Photophysics of Coordination Compounds II*; Springer: Berlin, 2007. (f) Nazeeruddin, M. K.; Grätzel, M. *Struct. Bonding (Berlin)* **2007**, *123*, 113−175.

(2) (a) Xiao, L.; Chen, Z.; Qu, B.; Luo, J.; Kong, S.; Gong, Q.; Kido, J. *Adv. Mater.* **2011**, *23*, 926−952. (b) Sasabe, H.; Kido, J. *Chem. Mater.* **2011**, *23*, 621−630. (c) Chen, Z.-Q.; Bian, Z.-Q.; Huang, C.-H. *Adv. Mater.* **2010**, *22*, 1534−1539. (d) Zhao, Q.; Li, F.; Huang, C. *Chem. Soc. Rev.* **2010**, *39*, 3007−3030. (e) Wong, W.-Y.; Ho, C.-L. *Coord. Chem. Rev.* **2009**, *253*, 1709−1758. (f) Wong, W.-Y.; Ho, C.-L. *J. Mater. Chem.* **2009**, *19*, 4457−4482. (g) Ulbricht, C.; Beyer, B.; Friebe, C.; Winter, A.; Schubert, U. S. *Adv. Mater.* **2009**, *21*, 4418−4441. (h) You, Y.; Park, S. Y. *Dalton Trans.* **2009**, 1267−1282.

(3) (a) Vezzu, D. A. K.; Deaton, J. C.; Jones, J. S.; Bartolotti, L.; Harris, C. F.; Marchetti, A. P.; Kondakova, M.; Pike, R. D.; Hou, S. *Inorg. Chem.* **2010**, *49*, 5107−5119. (b) Deaton, J. C.; Young, R. H.; Lenhard, J. R.; Rajeswaran, M.; Hou, S. *Inorg. Chem.* **2010**, *49*, 9151−9161. (c) Sajoto, T.; Djurovich, P. I.; Tamayo, A.; Oxgaard, J.; Goddard, W. A.; Thompson, M. E. *J. Am. Chem. Soc.* **2009**, *131*, 9813−9822. (d) *Highly Efficient OLEDs with Phosphorescent Materials*; Yersin, H., Ed.; Wiley−VCH Verlag GmbH & Co., KgaA: Weinheim, Germany, 2008. (e) Dedeian, K.; Shi, J.; Forsythe, E.; Morton, D. C. *Inorg. Chem.* **2007**, *46*, 1603−1611. (f) Sun, Y.; Borek, C.; Hanson, K.; Djurovich, P. I.; Thompson, M. E.; Brooks, J.; Brown, J. J.; Forrest, S. R. *Appl. Phys. Lett.* **2007**, *90*, 213503(1−3). (g) Sajoto, T.; Djurovich, P. I.; Tamayo, A.; Yousufuddin, M.; Bau, R.; Thompson, M. E. *Inorg. Chem.* **2005**, *44*, 7992−8003. (h) Dedeian, K.; Shi, J.; Shepherd, N.; Forsythe, E.; Morton, D. C. *Inorg. Chem.* **2005**, *44*, 4445−4447. (i) He, G.; Schneider, O.; Qin, D.; Zhou, X.; Pfeiffer, M.; Leo, K. J. *Appl. Phys.* **2004**, *95*, 5773−5777. (j) Tsuboyama, A.; Iwawaki, H.; Furugori, M.; Mukaide, T.; Kamatani, J.; Igawa, S.; Moriyama, T.; Miura, S.; Takiguchi, T.; Okada, S.; Hoshino, M.; Ueno, K. *J. Am. Chem. Soc.* **2003**, *125*, 12971−12979. (k) D'Andrade, B. W.; Thompson, M. E.; Forrest, S. R. *Adv. Mater.* **2002**, *14*, 147−151. (l) Brooks, J.; Babayan, Y.; Lamansky, S.; Djurovich, P. I.; Tsyba, I.; Bau, R.; Thompson, M. E. *Inorg. Chem.* **2002**, *41*, 3055−3066. (m) Lamansky, S.; Djurovich, P.; Murphy, D.; Abdel-Razzaq, F.; Lee, H. E.; Adachi, C.; Burrows, P. E.; Forrest, S. R.; Thompson, M. E. *J. Am. Chem. Soc.* **2001**, *123*, 4304−4312. (n) Wang, Y.; Herron, N.; Grushin, V. V.; LeCloux, D.; Petrov, V. *Appl. Phys. Lett.* **2001**, *79*,

dx.doi.org/10.1021/ic4002829 | *Inorg. Chem.* XXXX, XXX, XXX−XXX

449−451. (o) Lamansky, S.; Djurovich, P.; Murphy, D.; Abdel-Razzaq, F.; Kwong, R.; Tsyba, I.; Bortz, M.; Mui, B.; Bau, R.; Thompson, M. E. *Inorg. Chem.* **2001**, *40*, 1704−1711. (p) King, K. A.; Spellane, P. J.; Watts, R. J. *J. Am. Chem. Soc.* **1985**, *107*, 1431−1432.

(4) Barbieri, A.; Accorsi, G.; Armaroli, N. *Chem. Commun.* **2008**, 2185−2193.

(5) (a) Liu, Z.; Qayyum, M. F.; Wu, C.; Whited, M. T.; Djurovich, P. I.; Hodgson, K. O.; Hedman, B.; Solomon, E. I.; Thompson, M. E. *J. Am. Chem. Soc.* **2011**, *133*, 3700−3703. (b) Si, Z.; Li, J.; Li, B.; Liu, S.; Li, W. *J. Lumin.* **2009**, *129*, 181−186. (c) Zhang, Q.; Ding, J.; Cheng, Y.; Wang, L.; Xie, Z.; Jing, X.; Wang, F. *Adv. Funct. Mater.* **2007**, *17*, 2983−2990. (d) Jia, W.-L.; McCormick, T.; Tao, Y.; Lu, J.-P.; Wang, S. *Inorg. Chem.* **2005**, *44*, 5706−5712. (e) Koshevoy, I. O.; Chang, Y.-C.; Karttunen, A. J.; Haukka, M.; Pakkanen, T.; Chou, P.-T. *J. Am. Chem. Soc.* **2012**, *134*, 6564−6567.

(6) (a) Lippard, S. J.; Palenik, G. J. *Inorg. Chem.* **1971**, *10*, 1322−1324. (b) Grutsch, P. A.; Kutal, C. *J. Am. Chem. Soc.* **1979**, *101*, 4228−4233. (c) Fife, D. J.; Moore, W. M.; Morse, K. W. *Inorg. Chem.* **1984**, *23*, 1684−1691. (d) Kutal, C. *Coord. Chem. Rev.* **1990**, *99*, 213−252. (e) Kunkely, H.; Vogler, A. *Inorg. Chem. Commun.* **2002**, *5*, 112−114. (f) Sieger, M.; Vogler, C.; Klein, A.; Knödler, A.; Wanner, M.; Fiedler, J.; Záliš, S.; Snoeck, T. L.; Kaim, W. *Inorg. Chem.* **2005**, *44*, 4637−4643. (g) Kunkely, H.; Pawlowski, V.; Vogler, A. *Inorg. Chem. Commun.* **2008**, *11*, 1003−1005.

(7) (a) McMillin, D. R.; McNett, K. M. *Chem. Rev.* **1998**, *98*, 1201−1220. (b) Ford, P. C.; Cariati, E.; Bourassa, J. *Chem. Rev.* **1999**, *99*, 3625−3648. (c) Kalsani, V.; Schmittel, M.; Listorti, A.; Accorsi, G.; Armaroli, N. *Inorg. Chem.* **2006**, *45*, 2061−2067. (d) Armaroli, N.; Accorsi, G.; Cardinalli, F.; Listorti, A. *Top. Curr. Chem.* **2007**, *280*, 69−115. (e) Perruchas, S.; Le Goff, X. F.; Maron, S.; Maurin, I.; Guillen, F.; Garcia, A.; Gacoin, T.; Boilot, J.-P. *J. Am. Chem. Soc.* **2010**, *132*, 10967−10969. (f) Share, A. I.; Parimal, K.; Flood, A. H. *J. Am. Chem. Soc.* **2010**, *132*, 1665−1675. (g) Iwamura, M.; Watanabe, H.; Ishii, K.; Takeuchi, S.; Tahara, T. *J. Am. Chem. Soc.* **2011**, *133*, 7728−7736. (h) Nishikawa, M.; Nomoto, K.; Kume, S.; Nishihara, H. *J. Am. Chem. Soc.* **2012**, *134*, 10543−10553.

(8) (a) Zhang, Q.; Zhou, Q.; Cheng, Y.; Wang, L.; Ma, D.; Jing, X.; Wang, F. *Adv. Mater.* **2004**, *16*, 432−436. (b) Che, G.; Su, Z.; Li, W.; Chu, B.; Li, M.; Hu, Z.; Zhang, Z. *Appl. Phys. Lett.* **2006**, *89*, 10351(1−3). (c) Su, Z. S.; Che, G. B.; Li, W. L.; Su, W. M.; Li, M. T.; Chu, B.; Li, B.; Zhang, Z. Q.; Hu, Z. Z. *Appl. Phys. Lett.* **2006**, *88*, 213508(1−3). (d) Tsuboyama, A.; Kuge, K.; Furugori, M.; Okada, S.; Hoshino, M.; Ueno, K. *Inorg. Chem.* **2007**, *46*, 1992−2001. (e) Hsu, C.-W.; Lin, C.-C.; Chung, M.-W.; Chi, Y.; Lee, G.-H.; Chou, P.-T.; Chang, C.-H.; Chen, P.-Y. *J. Am. Chem. Soc.* **2011**, *133*, 12085−12099.

(9) Harkins, S. B.; Peters, J. C. *J. Am. Chem. Soc.* **2005**, *127*, 2030−2031.

(10) Deaton, J. C.; Switalski, S. C.; Kondakov, D. Y.; Young, R. H.; Pawlik, T. D.; Giesen, D. J.; Harkins, S. B.; Miller, A. J. M.; Mickenberg, S. F.; Peters, J. C. *J. Am. Chem. Soc.* **2010**, *132*, 9499−9508.

(11) Hashimoto, M.; Igawa, S.; Yashima, M.; Kawata, I.; Hoshino, M.; Osawa, M. *J. Am. Chem. Soc.* **2011**, *133*, 10348−10351.

(12) (a) Buckner, M. T.; Matthews, T. G.; Lytle, F. E.; McMillin, D. R. *J. Am. Chem. Soc.* **1979**, *101*, 5846−5848. (b) Blaskie, M. W.; McMillin, D. R. *Inorg. Chem.* **1980**, *19*, 3519−3522. (c) Song, D.; Jia, W. L.; Wu, G.; Wang, S. *Dalton Trans.* **2005**, 433−438. (d) Chou, C.-H.; Yeh, W.-Y.; Lee, G.-H.; Peng, S.-M. *Inorg. Chim. Acta* **2006**, *359*, 4139−4143. (e) Saito, K.; Arai, T.; Takahashi, N.; Tsukuda, T.; Tsubomura, T. *Dalton Trans.* **2006**, 4444−4448. (f) Wong, E.; Li, J.; Seward, C.; Wang, S. *Dalton Trans.* **2009**, 1776−1785. (g) Wei, F.; Fang, L.; Huang, Y. *Inorg. Chim. Acta* **2010**, *363*, 2600−2605. (h) Crestani, M. G.; Manbeck, G. F.; Brennessel, W. W.; McCormick, T. M.; Eidenberg, R. *Inorg. Chem.* **2011**, *50*, 7172−7188.

(13) (a) Rader, R. A.; McMillin, D. R.; Buckner, M. T.; Matthews, T. G.; Casadonte, D. J.; Lengel, R. K.; Whittaker, S. B.; Darmaon, L. M.; Lytle, F. E. *J. Am. Chem. Soc.* **1981**, *103*, 5906−5912. (b) McMillin, D. R.; Kirchhoff, J. R.; Goodwin, K. V. *Coord. Chem. Rev.* **1985**, *64*, 83−92. (c) Kirchhoff, J. R.; McMillin, D. R.; Robinson, W. R.; Powell, D. R.; McKenzie, A. T.; Chen, S. *Inorg. Chem.* **1985**, *24*, 3928−3933. (d) Dietrich-Buchecker, C. O.; Marnot, P. A.; Sauvage, J. P.; Kirchhoff, J. R.; McMillin, D. R. *J. Chem. Soc., Chem. Commun.* **1983**, 513−515. (e) Felder, D.; Nierengarten, J.-F.; Barigelletti, F.; Ventura, B.; Armaroli, N. *J. Am. Chem. Soc.* **2001**, *123*, 6291−6299. (f) Iwamura, M.; Takeuchi, S.; Tahara, T. *J. Am. Chem. Soc.* **2007**, *129*, 5248−5256.

(14) (a) Ma, Y.; Che, C.-M.; Chao, H.-Y.; Zhou, X.; Chan, W.-H.; Shan, J. *Adv. Mater.* **1999**, *11*, 852−857. (b) Zhang, L.; Li, B.; Su, Z. *J. Phys. Chem. C* **2009**, *113*, 13968−13973. (c) Min, J.; Zhang, Q.; Sun, W.; Cheng, Y.; Wang, L. *Dalton Trans.* **2011**, *40*, 686−693.

(15) (a) Armaroli, N.; Accorsi, G.; Holler, M.; Moudam, O.; Nierengarten, J.-F.; Zhou, Z.; Wegh, R. T.; Welter, R. *Adv. Mater.* **2006**, *18*, 1313−1316. (b) Moudam, O.; Kaeser, A.; Delavaux-Nicot, B.; Duhayon, C.; Holler, M.; Accorsi, G.; Armaroli, N.; Séguy, I.; Navarro, J.; Destruel, P.; Nierengarten, J.-F. *Chem. Commun.* **2007**, 3077−3079.

(16) (a) Barron, P. F.; Engelhardt, L. M.; Healy, P. C.; Kildea, J. D.; White, A. H. *Inorg. Chem.* **1988**, *27*, 1829−1834. (b) Niu, J.; Zhou, H.; Li, Z.; Xu, J.; Hu, S. *J. Org. Chem.* **2008**, *73*, 7814−7817. (c) Starosta, R.; Puchalska, M.; Cybińska, J.; Barys, M.; Mudring, A. V. *Dalton Trans.* **2011**, *40*, 2459−2468. (d) Balakrishna, M. S.; Suresh, D.; Rai, A.; Mague, J. T.; Panda, D. *Inorg. Chem.* **2010**, *49*, 8790−8801. (e) Starosta, R.; Florek, M.; Król, J.; Puchalska, M.; Kochel, A. *New J. Chem.* **2010**, *34*, 1441−1449. (f) Chen, J.-L.; Wu, B.; Gu, W.; Cao, X.-F.; Wen, H.-R.; Hong, R.; Liao, J.; Su, B.-T. *Transition Met. Chem.* **2011**, *36*, 379−385. (g) Xiao, Y.-L.; Jin, Q.-H.; Deng, Y.-H.; Li, Z.-F.; Yang, W.; Wu, M.-H.; Zhang, C.-L. *Inorg. Chem. Commun.* **2012**, *15*, 146−150. (h) Mauro, A. E.; Porta, C. C.; Ananias, S. R.; Sargentelli, V.; Santos, R. H.; De, A.; Gambardella, M. T.; Do, P. *J. Coord. Chem.* **1999**, *49*, 9−15. (i) Kickelbick, G.; Amirnasr, M.; Khalaji, A. D.; Dehghanpour, S. *Aust. J. Chem.* **2003**, *56*, 323−328.

(17) (a) Shi, Y.-J.; Chen, S.-J.; Huang, B.; Chen, X.-T.; Zhang, Y.; You, X.-Z. *J. Mol. Struct.* **2003**, *650*, 27−32. (b) Pettinari, C.; di Nicola, C.; Marchetti, F.; Pettinari, R.; Skelton, B. W.; Somers, N.; White, A. H.; Robinson, W. T.; Chierotti, M. R.; Gobetto, R.; Nervi, C. *Eur. J. Inorg. Chem.* **2008**, 1974−1984. (c) Chen, J.-L.; Cao, X.-F.; Gu, W.; Su, B.-T.; Zhang, F.; Wen, H.-R.; Hong, R. *Inorg. Chem. Commun.* **2012**, *15*, 65−68. (d) He, L.-H.; Chen, J.-L.; Zhang, F.; Cao, X.-F.; Tan, X.-Z.; Chen, X.-X.; Rong, G.; Luo, P.; Wen, H.-R. *Inorg. Chem. Commun.* **2012**, *21*, 125−128.

(18) (a) Potts, K. T. *Chem. Rev.* **1961**, *61*, 87−127. (b) Temple, C. Jr. *The Chemistry of Heterocyclic Compounds: Triazoles 1,2,4*; Wiley: New York, 1981; Vol. *37*. (c) Moulin, A.; Bibian, M.; Blayo, A.-L.; Habnouni, S. E.; Martinez, J.; Fehrentz, J.-A. *Chem. Rev.* **2010**, *110*, 1809−1827. (d) Haasnoot, J. G. *Coord. Chem. Rev.* **2000**, *200−202*, 131−185. (e) Meldal, M.; Tornoe, C. W. *Chem. Rev.* **2008**, *108*, 2952−3015. (f) Urankar, D.; Pinter, B.; Pevec, A.; De Proft, F.; Turel, I.; Kosmrlj, J. *Inorg. Chem.* **2010**, *49*, 4820−4829. (g) Hao, E.; Wang, Z.; Jiao, L.; Wang, S. *Dalton Trans.* **2010**, *39*, 2660−2666. (h) Schweinfurth, D.; Pattacini, R.; Strobel, S.; Sarkar, B. *Dalton Trans.* **2009**, 9291−9297. (i) Badeche, S.; Daran, J. C.; Ruiz, J.; Astruc, D. *Inorg. Chem.* **2008**, *47*, 4903−4908. (j) Li, Y.; Huffman, J. C.; Flood, A. H. *Chem. Commun.* **2007**, 2692−2694. (k) Krylova, V. A.; Djurovich, P. I.; Aronson, J. W.; Haiges, R.; Whited, M. T.; Thompson, M. E. *Organometallics* **2012**, *31*, 7983−7993.

(19) (a) Manbeck, G. F.; Brennessel, W. W.; Eisenberg, R. *Inorg. Chem.* **2011**, *50*, 3431−3441. (b) Manbeck, G. F.; Brennessel, W. W.; Evans, C. M.; Eisenberg, R. *Inorg. Chem.* **2010**, *49*, 2834−2843. (c) Bai, S.-Q.; Kwang, J. Y.; Koh, L. L.; Young, D. J.; Hor, T. S. A. *Dalton Trans.* **2010**, *39*, 2631−2636. (d) Monkowius, U.; Ritter, S.; König, B.; Zabel, M.; Yersin, H. *Eur. J. Inorg. Chem.* **2007**, 4597−4606. (e) Xiang, J.; Yin, Y. G.; Mei, P. *Inorg. Chem. Commun.* **2007**, *10*, 1168−1171.

(20) (a) Chou, P.-T.; Chi, Y. *Chem.—Eur. J.* **2007**, *13*, 380−395. (b) Chi, Y.; Chou, P.-T. *Chem. Soc. Rev.* **2007**, *36*, 1421−1431. (c) Chi, Y.; Chou, P.-T. *Chem. Soc. Rev.* **2010**, *39*, 638−655. (d) Chen, J.-L.; Wu, Y.-H.; He, L.-H.; Wen, H.-R.; Liao, J.; Hong, R. *Organometallics* **2010**, *29*, 2882−2891. (e) Chen, J.-L.; Chang, S.-Y.; Chi, Y.; Chen, K.; Cheng, Y.-M.; Lin, C.-W.; Lee, G.-H.; Chou, P.-T.;

dx.doi.org/10.1021/ic4002829 | *Inorg. Chem.* XXXX, XXX, XXX−XXX

Wu, C.-H.; Shih, P.-I; Shu, C.-F. *Chem. Asian J.* **2008**, *3*, 2112−2123. (f) Chen, J.-L.; Chi, Y.; Chen, K.; Cheng, Y.-M.; Chung, M.-W.; Yu, Y.-C.; Lee, G.-H.; Chou, P.-T.; Shu, C.-F. *Inorg. Chem.* **2010**, *49*, 823−832. (g) Wang, K.-W.; Chen, J.-L.; Cheng, Y.-M.; Chung, M.-W.; Hsieh, C.-C.; Lee, G.-H.; Chou, P.-T.; Chen, K.; Chi, Y. *Inorg. Chem.* **2010**, *49*, 1372−1383.

(21) (a) McCormick, T.; Jia, W.-L.; Wang, S. *Inorg. Chem.* **2006**, *45*, 147−155. (b) Chavan, S. S.; Sawant, S. K.; Sawant, V. A.; Lahiri, G. K. *Inorg. Chim. Acta* **2010**, *363*, 3359−3364. (c) Vorontsov, I. I.; Graber, T.; Kovalevsky, A. Y.; Novozhilova, I. V.; Gembicky, M.; Chen, Y.-S.; Coppens, P. *J. Am. Chem. Soc.* **2009**, *131*, 6566−6573. (d) Okubo, T.; Kitagawa, S.; Kondo, M.; Matsuzaka, H.; Ishii, T. *Angew. Chem., Int. Ed.* **1999**, *38*, 931−933. (e) Guerrero, J.; Cortez, L.; Lemus, L.; Farias, L.; Costamagna, J.; Pettinari, C.; Rossi, M.; Caruso, F. *Inorg. Chim. Acta* **2010**, *363*, 3809−3816. (f) Constable, E. C.; Housecroft, C. E.; Kopecky, P.; Schönhofer, E.; Zampese, J. A. *CrystEngComm* **2011**, *13*, 2742−2752.

(22) (a) Chen, L. X.; Shaw, G. B.; Novozhilova, I.; Liu, T.; Jennings, G.; Attenkofer, K.; Meyer, G. J.; Coppens, P. *J. Am. Chem. Soc.* **2003**, *125*, 7022−7034. (b) Chen, L. X.; Jenings, G.; Liu, T.; Gosztola, D. J.; Hessler, J. P.; Scaltrito, D. V.; Meyer, G. J. *J. Am. Chem. Soc.* **2002**, *124*, 10861−10867. (c) Sacksteder, L.; Zipp, A. P.; Brown, E. A.; Streich, J.; Demas, J. N.; DeGraff, B. A. *Inorg. Chem.* **1990**, *29*, 4335−4340. (d) Colombo, M. G.; Hauser, A.; Güdel, H. U. *Top. Curr. Chem.* **1994**, *171*, 143−171. (e) Weinstein, J. A.; van Slageren, J.; Stufkens, D. J.; Záliš, S.; George, M. W. *J. Chem. Soc., Dalton Trans.* **2001**, 2587−2592.

(23) (a) Cuttell, D. G.; Kuang, S. M.; Fanwick, P. E.; McMillin, D. R.; Walton, R. A. *J. Am. Chem. Soc.* **2002**, *124*, 6−7. (b) Kuang, S. M.; Cuttell, D. G.; McMillin, D. R.; Fanwick, P. E.; Walton, R. A. *Inorg. Chem.* **2002**, *41*, 3313−3322.

(24) Sakaki, S.; Mizutani, H.; Kase, Y.-I.; Inokuchi, K.-J.; Arai, T.; Hamada, T. *J. Chem. Soc., Dalton Trans.* **1996**, 1909−1914.

(25) (a) Smith, C. S.; Branham, C. W.; Marquardt, B. J.; Mann, K. R. *J. Am. Chem. Soc.* **2010**, *132*, 14079−14085. (b) Nishikawa, M.; Nomoto, K.; Kume, S.; Inoue, K.; Sakai, M.; Fujii, M.; Nishihara, H. *J. Am. Chem. Soc.* **2010**, *132*, 9579−9581. (c) Linfoot, C. L.; Richardson, P.; Hewat, T. E.; Moudam, O.; Forde, M. M.; Collins, A.; White, F.; Robertson, N. *Dalton Trans.* **2010**, *39*, 8945−8956. (d) Costa, R. D.; Tordera, D.; Ortí, E.; Bolink, H. J.; Schönle, J.; Graber, S.; Housecroft, C. E.; Constable, E. C.; Zampese, J. A. *J. Mater. Chem.* **2011**, *21*, 16108−16118. (e) Liu, X.; Sun, W.; Zou, L.; Xie, Z.; Li, X.; Lu, C.; Wang, L.; Cheng, Y. *Dalton Trans.* **2012**, *41*, 1312−1319. (f) Wada, A.; Zhang, Q.; Yasuda, T.; Takasu, I.; Enomoto, S.; Adachi, C. *Chem. Commun.* **2012**, *48*, 5340−5342.

(26) (a) Blasse, G.; McMillin, D. R. *Chem. Phys. Lett.* **1980**, *70*, 1−3. (b) Breddels, P. A.; Berdowski, P. A. M.; Blasse, G.; McMillin, D. R. *J. Chem. Soc., Faraday Trans.* **1982**, *78*, 595−601. (c) Kirchhoff, J. R.; Gamache, R. E., Jr.; Blaskie, M. W.; Del Paggio, A. A.; Lengel, R. K.; McMillin, D. R. *Inorg. Chem.* **1983**, *22*, 2380−2384. (d) Palmer, C. E. A.; McMillin, D. R. *Inorg. Chem.* **1987**, *26*, 3837−3840. (e) Siddique, Z. A.; Yamamoto, Y.; Ohno, T.; Nozaki, K. *Inorg. Chem.* **2003**, *42*, 6366−6378. (f) Asano, M. S.; Tomiduka, K.; Sekizawa, K.; Yamashita, K.-i.; Sugiura, K.-i. *Chem. Lett.* **2010**, *39*, 376−378. (g) Yersin, H.; Rausch, A. F.; Czerwieniec, R.; Hofbech, T.; Fischer, T. *Coord. Chem. Rev.* **2011**, *255*, 2622−2653. (h) Czerwieniec, R.; Yu, J.-B.; Yershin, H. *Inorg. Chem.* **2011**, *50*, 8293−8301. (i) Smith, C. S.; Mann, K. R. *J. Am. Chem. Soc.* **2012**, *134*, 8786−8789. (j) Yershi, H.; Czerwieniec, R.; Hupfer, A. *Proc. SPIE* **2012**, 843508. (k) Igawa, S.; Hashimoto, M.; Kawata, I.; Yashima, M.; Hoshino, M.; Osawa, M. *J. Mater. Chem. C* **2013**, *1*, 542−551. (l) Zink, D. M.; Bächle, M.; Baumann, T.; Nieger, M.; Kühn, M.; Wang, C.; Klopper, W.; Monkowius, U.; Hofbeck, T.; Yersin, H.; Bräse, S. *Inorg. Chem.* **2013**, *52*, 2292−2305.

(27) (a) Bauernschmitt, R.; Ahlrichs, R. *Chem. Phys. Lett.* **1996**, *256*, 454−464. (b) Casida, M. E.; Jamorski, C.; Casida, K. C.; Salahub, D. R. *J. Chem. Phys.* **1998**, *108*, 4439−4449. (c) Stratmann, R. E.; Scuseria, G. E.; Frisch, M. J. *J. Chem. Phys.* **1998**, *109*, 8218−8224.

(28) Perdew, J. P.; Burke, K.; Ernzerhof, M. *Phys. Rev. Lett.* **1996**, *77*, 3865−3868.

(29) Kubas, G. J.; Monzyk, B.; Crumbliss, A. L. *Inorg. Synth.* **1979**, *19*, 90−92.

(30) Díez, J.; Falagán, S.; Gamasa, P.; Gimeno, J. *Polyhedron* **1988**, *7*, 37−42.

(31) (a) Kubota, S.; Uda, M.; Nakagawa, T. *J. Heterocycl. Chem.* **1975**, *12*, 855−860. (b) Funabiki, K.; Noma, N.; Kuzuya, G.; Matsui, M.; Shibata, K. *J. Chem. Res., Miniprint* **1999**, 1301−1308. (c) Funabiki, K.; Noma, N.; Kuzuya, G.; Matsui, M.; Shibata, K. *J. Chem. Res., Synop.* **1999**, 300−301.

(32) Sheldrich, G. M. *SHELX-97, Program for Solution and Refinement of Crystal Structures*; University of Göttingen: Göttingen, Germany, 1997.

(33) (a) Crosby, G. A.; Demas, J. N. *J. Phys. Chem.* **1971**, *75*, 991−1024. (b) Xu, H.-B.; Chen, X.-M.; Zhang, Q.-S.; Zhang, L.-Y.; Chen, Z.-N. *Chem. Commun.* **2009**, 7318−7320.

(34) Frisch, M. J.; Trucks, G. W.; Schlegel, H. B.; Scuseria, G. E.; Robb, M. A.; Cheeseman, J. R.; Montgomery, J. A.; Jr.; Vreven, T.; Kudin, K. N.; Burant, J. C.; Millam, J. M.; Iyengar, S. S.; Tomasi, J.; Barone, V.; Mennucci, B.; Cossi, M.; Scalmani, G.; Rega, N.; Petersson, G. A.; Nakatsuji, H.; Hada, M.; Ehara, M.; Toyota, K.; Fukuda, R.; Hasegawa, J.; Ishida, M.; Nakajima, T.; Honda, Y.; Kitao, O.; Nakai, H.; Klene, M.; Li, X.; Knox, J. E.; Hratchian, H. P.; Cross, J. B.; Bakken, V.; Adamo, C.; Jaramillo, J.; Gomperts, R.; Stratmann, R. E.; Yazyev, O.; Austin, A. J.; Cammi, R.; Pomelli, C.; Ochterski, J. W.; Ayala, P. Y.; Morokuma, K.; Voth, G. A.; Salvador, P.; Dannenberg, J. J.; Zakrzewski, V. G.; Dapprich, S.; Daniels, A. D.; Strain, M. C.; Farkas, O.; Malick, D. K.; Rabuck, A. D.; Raghavachari, K.; Foresman, J. B.; Ortiz, J. V.; Cui, Q.; Baboul, A. G.; Clifford, S.; Cioslowski, J.; Stefanov, B. B.; Liu, G.; Liashenko, A.; Piskorz, P.; Komaromi, I.; Martin, R. L.; Fox, D. J.; Keith, T.; Al-Laham, M. A.; Peng, C. Y.; Nanayakkara, A.; Challacombe, M.; Gill, P. M. W.; Johnson, B.; Chen, W.; Wong, M. W.; Gonzalez, C.; Pople, J. A. *Gaussian 03, Revision D.02*; Gaussian, Inc.: Wallingford, CT, 2004.

(35) (a) Hohenberg, P.; Kohn, W. *Phys. Rev.* **1964**, *136*, B864−871. (b) Kohn, W.; Sham, L. J. *Phys. Rev.* **1965**, *140*, A1133−1138.

(36) (a) Barone, V.; Cossi, M.; Tomasi, J. *J. Chem. Phys.* **1997**, *107*, 3210−3221. (b) Cossi, M.; Scalmani, G.; Rega, N.; Barone, V. *J. Chem. Phys.* **2002**, *117*, 43−54.

(37) Bennett, M. A.; Bhargava, S. K.; Cheng, E. C.-C.; Lam, W. H.; Lee, T. K.-M.; Privér, S. H.; Wagler, J.; Willis, A. C.; Yam, V. W.-W. *J. Am. Chem. Soc.* **2010**, *132*, 7094−7103.

(38) (a) Hay, P. J.; Wadt, W. R. *J. Chem. Phys.* **1985**, *82*, 270−283. (b) Wadt, W. R.; Hay, P. J. *J. Chem. Phys.* **1985**, *82*, 284−298. (c) Hay, P. J.; Wadt, W. R. *J. Chem. Phys.* **1985**, *82*, 299−310.

(39) Francl, M. M.; Pietro, W. J.; Hehre, W. J.; Binkley, J. S.; Gordon, M. S.; DeFrees, D. J.; Pople, J. A. *J. Chem. Phys.* **1982**, *77*, 3654−3665.

(40) Pyykkö, P.; Runeberg, N.; Mendizabal, F. *Chem.—Eur. J.* **1997**, *3*, 1451−1457.

(41) Ros, P.; Schuit, G. C. A. *Theor. Chim. Acta* **1966**, *4*, 1−12.

(42) Lu, T.; Chen, F. *J. Comput. Chem.* **2012**, *33*, 580−592.